J. Fluid Mech. (1996), vol. 312, pp. 341–371

The generation of Tollmien–Schlichting waves by free-stream turbulence

By P. W. DUCK[1] A. I. RUBAN[2] AND C. N. ZHIKHAREV[3]

[1] Department of Mathematics, University of Manchester, Oxford Road, Manchester M13 9PL, UK

[2] Central Aerohydrodynamic Institute (TsAGI), Zhukovsky-3, Moscow reg., 140160, Russia

[3] Department of Mechanical Engineering and Mechanics, Lehigh University, Bethlehem, PA 18015, USA

(Received 27 October 1994 and in revised form 1 November 1995)

The phenomenon of Tollmien–Schlichting wave generation in a boundary layer by free-stream turbulence is analysed theoretically by means of asymptotic solution of the Navier–Stokes equations at large Reynolds numbers ($Re \to \infty$). For simplicity the basic flow is taken to be the Blasius boundary layer over a flat plate. Free-stream turbulence is taken to be uniform and thus may be represented by a superposition of vorticity waves. Interaction of these waves with the flat plate is investigated first. It is shown that apart from the conventional viscous boundary layer of thickness $O(Re^{-1/2})$, a 'vorticity deformation layer' of thickness $O(Re^{-1/4})$ forms along the flat-plate surface. Equations to describe the vorticity deformation process are derived, based on multiscale asymptotic techniques, and solved numerically. As a result it is shown that a strong singularity (in the form of a shock-like distribution in the wall vorticity) forms in the flow at some distance downstream of the leading edge, on the surface of the flat plate. This is likely to provoke abrupt transition in the boundary layer. With decreasing amplitude of free-stream turbulence perturbations, the singular point moves far away from the leading edge of the flat plate, and any roughness on the surface may cause Tollmien–Schlichting wave generation in the boundary layer. The theory describing the generation process is constructed on the basis of the 'triple-deck' concept of the boundary-layer interaction with the external inviscid flow. As a result, an explicit formula for the amplitude of Tollmien–Schlichting waves is obtained.

1. Introduction

Laminar–turbulent transition is an extraordinarily complicated process, consisting of a great number of competing events. The initial process is the transformation of external disturbances into internal instability oscillations of the boundary layer, taking the well-known form of Tollmien–Schlichting waves. In relatively quiet flows, the initial amplitude of these waves is insufficient to provoke immediate transition. Tollmien–Schlichting waves must first amplify in the boundary layer to trigger non-linear effects, characteristic of the transition process. Numerous experiments have clearly revealed that the extent of the amplification region, and hence the location of the 'transition point' on the body surface, is strongly dependent not only on the amplitude and/or the spectrum of external disturbances but also on their physical nature. Some of the disturbances easily penetrate into the boundary layer and

turn into Tollmien–Schlichting waves; others do not. To study these differences, the boundary-layer receptivity to external disturbances was proposed by Morkovin (1969) as a key problem in the laminar–turbulent transition process. The main objective of the investigations in this field is the determination of the amplitudes of generated Tollmien–Schlichting waves, and as a result the elucidation of which types of external disturbances can more easily provoke Tollmien–Schlichting waves.

From the mathematical point of view, the receptivity issue appears to be even more difficult than the stability problem. The latter is often associated with the solution of the Orr–Sommerfeld equation, while the former involves the solution of a boundary value problem for the Navier–Stokes equations. To date, direct numerical simulation of the full Navier–Stokes equations appears to be exceedingly difficult as far as unstable boundary-layer flows at high Reynolds number are concerned. On the other hand, asymptotic methods are well-suited for this type of problem.

The first paper where asymptotic techniques were used to solve a receptivity problem was published by Terent'ev (1981). His analysis was devoted to Tollmien–Schlichting waves generated by a vibrator installed in the boundary layer on the body surface. The classical experiments of Dryden (1956) and Schubauer & Skramsted (1948) were the first to generate Tollmien–Schlichting waves in a wind tunnel by means of a vibrating ribbon. This technique is simple, and still used to provoke Tollmien–Schlichting waves. In the theoretical analysis of Terent'ev (1981), the role of the vibrator was modelled by a short, flexible section of the body surface, and to describe the Tollmien–Schlichting wave generation process, he used an unsteady version of triple-deck theory. It was shown previously by Lin (1946), Smith (1979) and Zhuk & Ryzhov (1980) that this provides the asymptotic description of Tollmien–Schlichting waves near the lower branch of the boundary-layer neutral stability curve. To satisfy the restrictions of triple-deck theory, the (non-dimensional) longitudinal extent ℓ of the vibrating part of the body surface was chosen to be $\ell = O(Re^{-3/8})$, while the (non-dimensional) frequency of oscillation $\omega = O(Re^{1/4})$, where Re is Reynolds number. As a result of this analysis, an explicit formula may be obtained for the amplitude of a Tollmien–Schlichting wave propagating in the boundary layer, downstream of the vibrator. This problem was extended into the nonlinear regime by Duck (1985), a study which indicated that finite-time breakdowns are a common occurrence in flows of this type. This latter work was extended into the three-dimensional regime by Duck (1990).

The problem of Tollmien–Schlichting wave generation by sound was first considered by Fedorov (1982), who analysed the interaction of acoustic waves with a growing boundary layer on a flat-plate surface. As a result it was shown that the non-uniformity of the boundary-layer flow, being especially significant near the leading edge, leads to the scattering of acoustic waves into instability waves of the boundary layer. The generation of Tollmien–Schlichting waves via the interaction of an external acoustic field with a wall roughness element was investigated by Ruban (1984) and independently by Goldstein (1985). Effective transformation of external disturbances into Tollmien–Schlichting waves is possible if resonance conditions are satisfied. For boundary-layer flows, the resonance between external disturbances and internal instability waves supposes coincidence not only of frequencies, but also of wavenumbers. This coincidence may easily be achieved in the problem considered by Terent'ev (1981) since the frequency of the vibrating section of the surface and its extent may be chosen independently. If an acoustic wave plays the role of the external perturbation, it is possible to choose its (non-dimensional) frequency to be $\omega = O(Re^{1/4})$, but then the wavelength of the disturbance is much larger than

that appropriate to Tollmien–Schlichting waves. In order to introduce the necessary lengthscale into the problem, Ruban (1984) and Goldstein (1985) supposed that the body surface was not absolutely smooth, and the acoustic wave interacts with a stationary disturbance provoked in the boundary layer by wall roughness. The effective generation of Tollmien–Schlichting waves was shown to take place if the (non-dimensional) length ℓ of the roughness is $O(Re^{-3/8})$. Similar ideas have been used by Ryzhov & Timpfeev (1995), who analysed the interaction between a single vortex and local roughness. The above analysis was for a linearized, steady basic flow, together with a linearized unsteady perturbation. This problem was extended to the case of a non-linear steady, basic flow, subject to linearised unsteady perturbations by Bodonyi *et al.* (1989), whilst the fully non-linear version of this problem was treated by Duck (1988), who showed that finite-time breakdowns were likely for this problem, also.

An extremely important paper by Goldstein (1983) considered how boundary-layer growth effects, interacting with acoustic free-stream waves could also account for the seeding of Tollmien–Schlichting waves, without the need for any form of flat-plate surface distortion. This paper showed how initially decaying eigensolutions then developed progressively smaller wavelengths downstream of the plate leading edge, and eventually the growing Tollmien–Schlichting mode is triggered. The work of Goldstein & Leib (1993*a*, *b*) and Goldstein, Leib & Cowley (1992) is also relevant in this context.

It is well known from experimental observations that the laminar–turbulent transition process is sensitive not only to wall vibrations and/or acoustic fields, but is also strongly affected by free-stream turbulence. In the present paper Tollmien–Schlichting waves generated in boundary layers by external turbulent perturbations are analysed theoretically. The most 'aggressive' part of the turbulent spectrum, corresponding to vorticity waves with (non-dimensional) frequency $\omega = O(Re^{1/4})$ is considered. Since the vorticity waves propagate along the boundary layer with the free-stream velocity, their (non-dimensional) wavelength $\lambda = O(Re^{-1/4})$ again appears to be much greater than the wavelength of Tollmien–Schlichting waves. For this reason it may be anticipated that wall irregularities, even if they are small, are very important for the Tollmien–Schlichting wave generation process. In the present paper the analysis is carried out for a single wall roughness element with (non-dimensional) longitudinal extent $\ell = O(Re^{-3/8})$. Thus the formulation of the problem (§2) resembles that considered by Ruban (1984) and Goldstein (1985) for acoustic waves. The essential difference between acoustic and vorticity waves is that the latter do not create a pressure gradient at the outer edge of the boundary layer (assuming linear perturbations) and so do not provoke flow oscillations inside the boundary layer.

The analysis is carried out for small-amplitude (ϵ) of free-stream turbulence perturbations. The paper consists of two major parts. In §3 the process of vorticity waves deforming near the flat-plate surface and their subsequent penetration into the boundary layer is investigated. The problem was first considered by Hunt & Graham (1978), who supposed that the free-stream turbulence is uniform and so may be represented as a superposition of sinusoidal vorticity waves. Since the corresponding velocity field does not automatically satisfy the impermeability condition on the flat-plate surface, the flow near the flat plate must be considered. Hunt & Graham (1978) carried out their analysis based on the inviscid Euler equations. With the assumption that the vorticity field is not influenced by the wall and so is just the same as in the free-stream, it is shown that a vortex layer forms along the flat plate. Its thickness is of the same order of magnitude as the (non-dimensional) wavelength of the vorticity

wave, namely $\lambda = O(Re^{-1/4})$. Near the bottom of this layer, velocity fluctuations take on their maximum amplitudes, but the pressure gradient remains zero. Investigation of the flow inside the Blasius viscous boundary layer of thickness $O(Re^{-1/2})$ was carried out by Guliaev *et al.* (1989). They found that velocity perturbations decay rapidly within an intermediate viscous layer located near the outer edge of the Blasius boundary layer. As a result of their analysis Guliaev *et al.* (1989) arrived at the conclusion that turbulent perturbations do not penetrate into the bulk of the boundary layer and for that reason Tollmien–Schlichting waves cannot be generated.

In the present paper we will show that this conclusion is somewhat premature. As was pointed out by Kerschen (1991), generation of Tollmien–Schlichting waves may be associated not only with a penetration of external perturbations into the boundary layer and subsequent interaction of the boundary-layer oscillations with wall roughness, which is the case, for example, for the scattering of acoustic perturbations into Tollmien–Schlichting waves. Tollmien–Schlichting waves may be also generated from the interaction of oncoming free-stream oscillations with stationary perturbations produced by wall roughness outside the boundary layer. While such an interaction is known to be very weak for other applications of triple-deck theory when all the notable perturbations are concentrated in the near-wall viscous sublayer (see, for example, Sychev *et al.* 1987), it might become the leading-order process if the boundary layer is exposed to external flow vorticity waves. Another effect that, despite its importance, has not been considered in previous studies is the vorticity field deformation near a rigid-body surface. It leads not only to the amplification of velocity oscillations at the outer edge of the boundary layer, but also to the formation of pressure oscillations in the inviscid turbulence deformation layer and, consequently, in the viscous flow inside the boundary layer. In §3 it is shown that the flow structure in the vicinity of the flat plate is four-tiered. It consists of (i) an inviscid vortex layer which will also be called the vorticity or turbulence deformation layer, its (non-dimensional) thickness being $O(Re^{-1/4})$, (ii) the Blasius boundary layer with thickness $O(Re^{-1/2})$, (iii) a near-wall Stokes sublayer where $y = O(Re^{-5/8})$ and (iv) an intermediate oscillatory shear layer of thickness $\Delta y = O[(Re \log Re)^{-1/2}]$ between the inviscid vortex layer and the Blasius boundary layer.

The process of vorticity field deformation in the vortex layer is described by the Helmholtz equation (3.10) (all quantities are defined fully in §3)

$$\frac{\partial \omega_1}{\partial \bar{X}} + \bar{U}_1 \frac{\partial \omega_1}{\partial \bar{x}} + \bar{V}_1 \frac{\partial \omega_1}{\partial \bar{y}} = 0. \tag{1.1}$$

Here the role of time is played by the 'slow' spatial variable $\bar{X}$ measuring the distance along the flat plate on the scale which is ϵ^{-1} times longer than the wavelength of the vorticity wave. If the amplitude ϵ of free-stream perturbations is $O(Re^{-1/4})$, then at a finite distance from the leading edge, this process leads to a singularity in the flow outside the boundary layer, which may be anticipated to cause an abrupt laminar–turbulent transition in the boundary layer.

On the other hand, if the amplitude of external turbulence perturbations is small enough, the singular point moves downstream and the process of Tollmien–Schlichting wave generation appears to be important. This is investigated in §4 where the flow in the vicinity of wall roughness is considered on the basis of triple-deck theory. It is interesting that in the present case nonlinear effects leading to Tollmien–Schlichting wave generation take place in the upper deck of the triple-deck structure, while the near-wall viscous sublayer flow remains linear. It is also interesting that despite the differences in the physical processes leading to the generation of Tollmien–Schlichting

FIGURE 1. Basic layout.

waves by external vorticity waves on the one hand and by wall vibrator, considered by, for example, Terent'ev (1981, 1984), on the other hand, the mathematical problems describing the processes may be reduced to one another. Therefore the results of Terent'ev's (1981, 1984) analysis may be directly used for our purposes. In addition to that it is also shown in §5 that an explicit general formula may be derived for the amplitude of Tollmien–Schlichting waves generated via the interaction of external turbulence perturbations, with stationary boundary-layer perturbations around the roughness.

2. Formulation of the problem

Consider the incompressible viscous fluid flow over a semi-infinite flat plate aligned with the mean velocity vector upstream of the flat plate (figure 1). We denote the free-stream velocity value by U_∞ and pressure by p_∞. Suppose that there is a small roughness element on the plate surface, a distance L downstream from the leading edge, and introduce Cartesian coordinates (Lx, Ly), where x is measured along the flat plate from its leading edge and y is the normal coordinate. Let $(U_\infty u, U_\infty v)$ be the velocity components in this coordinate system, and $p_\infty + \rho U_\infty^2 p$ be pressure. The density ρ of the fluid and the viscosity coefficient μ are both assumed to be constant. With time defined as $(L/U_\infty)t$ the Navier–Stokes equations take the form

$$\left.\begin{aligned} &\frac{\partial u}{\partial t} + u\frac{\partial u}{\partial x} + v\frac{\partial u}{\partial y} = -\frac{\partial p}{\partial x} + \frac{1}{Re}\left(\frac{\partial^2 u}{\partial x^2} + \frac{\partial^2 u}{\partial y^2}\right), \\ &\frac{\partial v}{\partial t} + u\frac{\partial v}{\partial x} + v\frac{\partial v}{\partial y} = -\frac{\partial p}{\partial y} + \frac{1}{Re}\left(\frac{\partial^2 v}{\partial x^2} + \frac{\partial^2 v}{\partial y^2}\right), \\ &\frac{\partial u}{\partial x} + \frac{\partial v}{\partial y} = 0, \end{aligned}\right\} \tag{2.1}$$

where the Reynolds number

$$Re = \frac{\rho U_\infty L}{\mu}$$

is taken to be large in the following analysis.

We represent the solution for (2.1) in the free-stream by the asymptotic expansions

$$\left.\begin{aligned} u &= 1 + \epsilon\bar{u}_1(\bar{t}, \bar{x}, \bar{y}) + \epsilon^2\bar{u}_2(\bar{t}, \bar{x}, \bar{y}) + \ldots, \\ v &= \epsilon\bar{v}_1(\bar{t}, \bar{x}, \bar{y}) + \epsilon^2\bar{v}_2(\bar{t}, \bar{x}, \bar{y}) + \ldots, \\ p &= \epsilon\bar{p}_1(\bar{t}, \bar{x}, \bar{y}) + \epsilon^2\bar{p}_2(\bar{t}, \bar{x}, \bar{y}) + \ldots, \end{aligned}\right\} \tag{2.2}$$

where the scaling $Re^{-1/4}$ is used for both time and the spatial coordinates, namely

$$t = Re^{-1/4}\bar{t}, \quad x = Re^{-1/4}\bar{x}, \quad y = Re^{-1/4}\bar{y}. \tag{2.3}$$

This satisfies the resonance condition for the external perturbation frequency to coincide with that of internal Tollmien–Schlichting waves near the lower branch of the boundary-layer stability curve. The amplitude of the perturbations ϵ is assumed to be small compared with unity.

Substitution of (2.2), (2.3) into (2.1), to leading order leads to the linearized Euler equations

$$\frac{\partial \bar{u}_1}{\partial \bar{t}} + \frac{\partial \bar{u}_1}{\partial \bar{x}} = -\frac{\partial \bar{p}_1}{\partial \bar{x}}, \quad \frac{\partial \bar{v}_1}{\partial \bar{t}} + \frac{\partial \bar{v}_1}{\partial \bar{x}} = -\frac{\partial \bar{p}_1}{\partial \bar{y}}, \quad \frac{\partial \bar{u}_1}{\partial \bar{x}} + \frac{\partial \bar{v}_1}{\partial \bar{y}} = 0. \tag{2.4}$$

It follows from (2.4) that the vorticity, defined by

$$\bar{\omega}_1 = \frac{\partial \bar{v}_1}{\partial \bar{x}} - \frac{\partial \bar{u}_1}{\partial \bar{y}}, \tag{2.5}$$

is function of $\xi = \bar{x} - \bar{t}$ and $\bar{y}$ only.

Since the free-stream turbulence is taken to be uniform, the vorticity field may be expressed as a superposition of periodic functions of ξ and $\bar{y}$:

$$\bar{\omega}_1 = \sum_{\alpha,\beta} \omega_1^0 e^{i(\alpha\xi + \beta\bar{y})} + \text{c.c.}, \tag{2.6}$$

ω_1^0 being the amplitude of the corresponding harmonic and α, β denote the (real) wavenumbers in the $\bar{x}$- and $\bar{y}$-directions respectively, and where c.c. denotes the complex conjugate.

It follows from (2.5), (2.6) and the continuity equation (2.4) that the velocity components in the free-stream flow take the form

$$\left.\begin{aligned} \bar{u}_1 &= \sum_{\alpha,\beta} \frac{i\beta\omega_1^0}{\alpha^2 + \beta^2} e^{i(\alpha\xi + \beta\bar{y})} + \text{c.c.}, \\ \bar{v}_1 &= -\sum_{\alpha,\beta} \frac{i\alpha\omega_1^0}{\alpha^2 + \beta^2} e^{i(\alpha\xi + \beta\bar{y})} + \text{c.c.}. \end{aligned}\right\} \tag{2.7}$$

Substitution of (2.7) into (2.4) leads to the conclusion that there can be no pressure gradient in the free-stream to leading order, and so

$$\frac{\partial \bar{p}_1}{\partial \bar{x}} = \frac{\partial \bar{p}_1}{\partial \bar{y}} = 0.$$

The quadratic terms in (2.2) are described by

$$\left.\begin{aligned} \frac{\partial \bar{u}_2}{\partial \bar{t}} + \frac{\partial \bar{u}_2}{\partial \bar{x}} + \bar{u}_1 \frac{\partial \bar{u}_1}{\partial \bar{x}} + \bar{v}_1 \frac{\partial \bar{u}_1}{\partial \bar{y}} &= -\frac{\partial \bar{p}_2}{\partial \bar{x}}, \\ \frac{\partial \bar{v}_2}{\partial \bar{t}} + \frac{\partial \bar{v}_2}{\partial \bar{x}} + \bar{u}_1 \frac{\partial \bar{v}_1}{\partial \bar{x}} + \bar{v}_1 \frac{\partial \bar{v}_1}{\partial \bar{y}} &= -\frac{\partial \bar{p}_2}{\partial \bar{y}}, \\ \frac{\partial \bar{u}_2}{\partial \bar{x}} + \frac{\partial \bar{v}_2}{\partial \bar{y}} &= 0. \end{aligned}\right\} \tag{2.8}$$

The solution of (2.8) depends on the specific form of (2.6). If 'convective gusts' are considered, where the vorticity field is represented by just one harmonic, we may write

$$\bar{\omega}_1 = \omega_1^0 e^{i(\alpha\xi + \beta\bar{y})} + \text{c.c.},$$

and then the pressure gradients are both zero in the second approximation also, i.e.

$$\frac{\partial \bar{p}_2}{\partial \bar{x}} = \frac{\partial \bar{p}_2}{\partial \bar{y}} = 0.$$

On the other hand, if we take the combination of two symmetrical harmonics

$$\bar{\omega}_1 = \omega_1^0 e^{i(\alpha\xi+\beta\bar{y})} + \omega_1^0 e^{i(\alpha\xi-\beta\bar{y})} + \text{c.c.},$$

where the amplitude ω_1^0 is real, then the pressure gradient takes the form

$$\frac{\partial \bar{p}_2}{\partial \bar{x}} = -\frac{8(\omega_1^0)^2\alpha\beta^2}{(\alpha^2+\beta^2)^2}\sin 2\alpha\xi, \quad \frac{\partial \bar{p}_2}{\partial \bar{y}} = -\frac{8(\omega_1^0)^2\beta\alpha^2}{(\alpha^2+\beta^2)^2}\sin 2\beta\bar{y}.$$

It will be shown in §3 that the vorticity field deformation near the surface leads to a non-zero pressure gradient $\partial\bar{p}_2/\partial\bar{x}$ at the outer edge of the boundary layer, even if the free-stream perturbations take the form of 'convective gusts'. In the vicinity of the wall roughness both longitudinal velocity components outside the boundary layer and the pressure gradient inside the boundary layer oscillate in time with frequency $\omega = Re^{1/4}\alpha$, but it is necessary to keep in mind that the amplitude of the velocity oscillations outside the boundary layer is $O(\epsilon)$, while the pressure oscillations have an amplitude $O(\epsilon^2)$, which therefore cause only $O(\epsilon^2)$ velocity oscillations inside the boundary layer.

In order that Tollmien–Schlichting waves be generated, these temporal oscillations must be accompanied by spatial perturbations in the boundary layer, with appropriate longitudinal extent. If the extent is taken to be $O(Re^{-3/8})$, then the wavenumber coincides with that of Tollmien–Schlichting waves. Thus resonance conditions will be satisfied if the wall roughness has the form

$$y = Re^{-5/8}F\left(\frac{x-1}{Re^{-3/8}}\right), \tag{2.9}$$

where generally the function $F = O(1)$ for finite values of its argument. Analysis of the flow in the vicinity of the roughness is presented in §4.

3. Flow behaviour upstream of the roughness

Since the free-stream velocity field (2.7) does not satisfy the impermeability condition on the flat-plate surface, a vortex boundary layer forms near the wall. It occupies a narrow strip along the flat plate, with thickness of the same order as the wavelength of the free-stream vorticity wave, namely $y = O(Re^{-1/4})$. Two physical processes must be taken into account in the analysis of this region. First, there is an almost immediate modification of the velocity field owing to the impermeability condition and, second, a very slow process of deformation of the vorticity field, associated with a slow movement of fluid particles with respect to the free-stream mean velocity.

For these reasons, the solution in the vortex layer (region 1 in figure 2) may be expressed in the form of the following multiscale asymptotic expansions:

$$\left.\begin{aligned} u &= 1 + \epsilon\bar{U}_1(\bar{t},\bar{x},\bar{X},\bar{y}) + \epsilon^2\bar{U}_2(\bar{t},\bar{x},\bar{X},\bar{y}) + \ldots, \\ v &= \epsilon\bar{V}_1(\bar{t},\bar{x},\bar{X},\bar{y}) + \epsilon^2\bar{V}_2(\bar{t},\bar{x},\bar{X},\bar{y}) + \ldots, \\ p &= \epsilon\bar{P}_1(\bar{t},\bar{x},\bar{X},\bar{y}) + \epsilon^2\bar{P}_2(\bar{t},\bar{x},\bar{X},\bar{y}) + \ldots, \end{aligned}\right\} \tag{3.1}$$

where fast variables $\bar{t},\bar{x},\bar{y}$ are just the same as in the free-stream flow, namely (2.3),

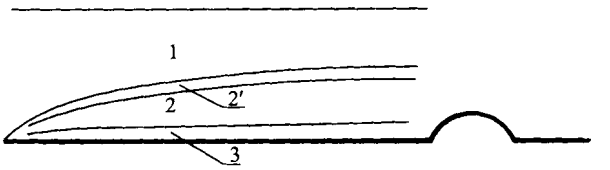

FIGURE 2. Layout of asymptotic regions; the characteristic thicknesses of the regions are 1: $O(Re^{-1/4})$, 2: $O(Re^{-1/2})$, 3: $O(Re^{-5/8})$, 2': $O(Re^{-1/2}\,[\log Re]^{-1/2})$.

while the slow variable $\overline{X}$ is defined by

$$\overline{X} = \epsilon Re^{1/4} x. \tag{3.2}$$

Substitution of (3.1) into the Navier–Stokes equations (2.1) leads to the linearized Euler equations

$$\frac{\partial \overline{U}_1}{\partial \bar{t}} + \frac{\partial \overline{U}_1}{\partial \bar{x}} = -\frac{\partial \overline{P}_1}{\partial \bar{x}}, \quad \frac{\partial \overline{V}_1}{\partial \bar{t}} + \frac{\partial \overline{V}_1}{\partial \bar{x}} = -\frac{\partial \overline{P}_1}{\partial \bar{y}}, \quad \frac{\partial \overline{U}_1}{\partial \bar{x}} + \frac{\partial \overline{V}_1}{\partial \bar{y}} = 0. \tag{3.3}$$

Cross-differentiation of the first two equations shows that the vorticity

$$\omega_1 = \frac{\partial \overline{V}_1}{\partial \bar{x}} - \frac{\partial \overline{U}_1}{\partial \bar{y}} \tag{3.4}$$

is a function of $\overline{X}, \xi = \bar{x} - \bar{t}$ and $\bar{y}$ only.

If ω_1 were known, the velocity field could be determined as follows. Based on the continuity equation in (3.3), we introduce the stream function ψ_1 such that

$$\overline{U}_1 = \frac{\partial \psi_1}{\partial \bar{y}}, \quad \overline{V}_1 = -\frac{\partial \psi_1}{\partial \bar{x}}. \tag{3.5}$$

Substitution of (3.5) into (3.4) leads to the equation

$$\frac{\partial^2 \psi_1}{\partial \bar{x}^2} + \frac{\partial^2 \psi_1}{\partial \bar{y}^2} = -\omega_1, \tag{3.6}$$

which must be subject to the impermeability condition on the flat plate surface

$$\psi_1 = 0 \quad \text{at} \quad \bar{y} = 0 \tag{3.7}$$

The matching condition with the longitudinal velocity component in the free-stream flow (2.7) leads to

$$\frac{\partial \psi_1}{\partial \bar{y}} = \sum_{\alpha,\beta} \frac{\mathrm{i}\beta\omega_1^0}{\alpha^2 + \beta^2} \mathrm{e}^{\mathrm{i}(\alpha\xi + \beta\bar{y})} + \text{c.c.} \quad \text{as} \quad \bar{y} \to \infty. \tag{3.8}$$

In order to find the vorticity ω_1, consider the second-order equations in the vortex layer, namely

$$\left.\begin{aligned} &\frac{\partial \overline{U}_2}{\partial \bar{t}} + \frac{\partial \overline{U}_2}{\partial \bar{x}} + \frac{\partial \overline{U}_1}{\partial \overline{X}} + \overline{U}_1 \frac{\partial \overline{U}_1}{\partial \bar{x}} + \overline{V}_1 \frac{\partial \overline{U}_1}{\partial \bar{y}} = -\frac{\partial \overline{P}_2}{\partial \bar{x}} - \frac{\partial \overline{P}_1}{\partial \overline{X}}, \\ &\frac{\partial \overline{V}_2}{\partial \bar{t}} + \frac{\partial \overline{V}_2}{\partial \bar{x}} + \frac{\partial \overline{V}_1}{\partial \overline{X}} + \overline{U}_1 \frac{\partial \overline{V}_1}{\partial \bar{x}} + \overline{V}_1 \frac{\partial \overline{V}_1}{\partial \bar{y}} = -\frac{\partial \overline{P}_2}{\partial \bar{y}}, \\ &\frac{\partial \overline{U}_1}{\partial \overline{X}} + \frac{\partial \overline{U}_2}{\partial \bar{x}} + \frac{\partial \overline{V}_2}{\partial \bar{y}} = 0. \end{aligned}\right\} \tag{3.9}$$

The expansions (3.1) are assumed to be uniformly valid with respect to $\overline{X}$. For this reason we seek the solution in which not only $\overline{U}_1, \overline{V}_1$, but also $\overline{U}_2, \overline{V}_2$ are functions of $\xi = \overline{x} - \overline{t}, \overline{X}$ and $\overline{y}$. Taking this restriction into account, we can easily obtain from the momentum equations in (3.3) that

$$\frac{\partial \overline{P}_1}{\partial \overline{x}} = \frac{\partial \overline{P}_1}{\partial \overline{y}} = 0.$$

The first two terms in both the longitudinal and the lateral momentum equations in (3.9) cancel for the same reason, and cross-differentiation of the residual terms leads to the vorticity evolution equation

$$\frac{\partial \omega_1}{\partial \overline{X}} + \overline{U}_1 \frac{\partial \omega_1}{\partial \xi} + \overline{V}_1 \frac{\partial \omega_1}{\partial \overline{y}} = 0. \tag{3.10}$$

This must be solved subject to the following initial condition at the leading edge of the flat plate:

$$\omega_1 = \sum_{\alpha,\beta} \omega_1^0 e^{i(\alpha\xi + \beta\overline{y})} + \text{c.c.} \quad \text{at} \quad \overline{X} = 0, \tag{3.11}$$

where the vorticity evolves from the unperturbed free-stream state (2.6).

The boundary value problem is then represented by a combination of (3.6)–(3.8) and (3.10)–(3.11). In order to describe the Tollmien–Schlichting wave generation process, we need to know the solution in the vortex layer near the roughness location $x = 1$. In accordance with (3.2), the slow variable $\overline{X}$ at this point is $\overline{X} = \epsilon Re^{1/4}$. Therefore, depending on the ratio of the free-stream perturbation amplitude ϵ and its first critical value $\epsilon^* = Re^{-1/4}$, the solution for small, finite or large values of $\overline{X}$ may be required.

Suppose, first, that ϵ is small compared with ϵ^*. In that case the solution for (3.5)–(3.8), (3.10), (3.11) may be expressed in the form of Taylor expansions

$$\omega_1 = \omega_{10}(\xi, \overline{y}) + \overline{X}\omega_{11}(\xi, \overline{y}) + \ldots, \tag{3.12}$$

$$\psi_1 = \psi_{10}(\xi, \overline{y}) + \overline{X}\psi_{11}(\xi, \overline{y}) + \ldots \tag{3.13}$$

Since equation (3.10) is nonlinear, the solution must be dependent on the nature of the superposition in (2.6). If a simple 'convective gust' flow is considered then

$$\omega_{10} = \omega_1^0 e^{i(\alpha\xi + \beta\overline{y})} + \text{c.c.}, \tag{3.14}$$

$$\psi_{10} = \omega_1^0 \left[\frac{e^{i\beta\overline{y}} - e^{-\alpha\overline{y}}}{\alpha^2 + \beta^2}\right] e^{i\alpha\xi} + \text{c.c.} \tag{3.15}$$

and

$$\omega_{11} = -(i\alpha^2 - \alpha\beta)\frac{(\omega_1^0)^2}{\alpha^2 + \beta^2} e^{-\alpha\overline{y}} e^{i(2\alpha\xi + \beta\overline{y})} - (i\alpha^2 + \alpha\beta)\frac{\omega_1^0 \overline{\omega_1^0}}{\alpha^2 + \beta^2} e^{-\alpha\overline{y}} e^{i\beta\overline{y}} + \text{c.c.} \tag{3.16}$$

$$\psi_{11} = \frac{i\alpha}{(\alpha - i\beta)}\frac{\omega_1^0 \overline{\omega_1^0}}{(\alpha^2 + \beta^2)}\left[e^{(i\beta - \alpha)\overline{y}} - 1\right] + \frac{\alpha}{(\beta + 3i\alpha)}\frac{(\omega_1^0)^2}{(\alpha^2 + \beta^2)}\left[e^{(i\beta - \alpha)\overline{y}} - e^{-2\alpha\overline{y}}\right] e^{i2\alpha\xi} + \text{c.c.} \tag{3.17}$$

such that the pressure gradient appears to be

$$\frac{\partial \overline{P}_2}{\partial \overline{x}} = -\frac{\alpha(\omega_1^0)^2 e^{2i\alpha\xi}}{\alpha^2+\beta^2}\left[\frac{2\alpha}{\beta+3i\alpha}e^{-2\alpha\overline{y}} + \left(\frac{i\beta-\alpha}{\beta+3i\alpha}+\frac{i\alpha-\beta}{\alpha-i\beta}\right)e^{(i\beta-\alpha)\overline{y}}\right] + \text{c.c.} \tag{3.18}$$

This tends to zero at the outer edge of the vortex layer, as $\overline{y} \to \infty$, and takes the form

$$\frac{\partial \overline{P}_2}{\partial \overline{x}} = \frac{2\alpha^2(\alpha+i\beta)^2(\omega_1^0)^2}{(\beta+3i\alpha)(\alpha^2+\beta^2)^2}e^{i2\alpha\xi} + \text{c.c.} \tag{3.19}$$

near the bottom of the vortex layer.

It is now routine to extend the above series in $\overline{X}$ to higher order; however for finite values of $\overline{X}$ the solution of (3.5)–(3.8), (3.10) and (3.11) must be obtained numerically.

Two numerical approaches were adopted. The first was a spectral scheme, based on a Fourier series representation in the ξ-direction, which automatically 'built in' the periodic nature of the flow. We write

$$\omega_1(\overline{X},\overline{y},\xi) = \sum_{n=-\infty}^{\infty} \hat{\omega}_n(\overline{y},\overline{X})e^{i\alpha n\xi}, \tag{3.20}$$

$$\psi_1(\overline{X},\overline{y},\xi) = \sum_{n=-\infty}^{\infty} \hat{\psi}_n(\overline{y},\overline{X})e^{i\alpha n\xi}, \tag{3.21}$$

and so (3.6) reduces simply to

$$\hat{\omega}_n = \hat{\psi}_{n\overline{y}\overline{y}} - \alpha^2 n^2 \hat{\psi}_n, \tag{3.22}$$

whilst (3.10) may then be written in the form

$$\frac{\partial \hat{\omega}_n}{\partial \overline{X}} + \sum_{m=-\infty}^{\infty} im\left[\hat{\psi}_{n-m\overline{y}}\hat{\omega}_m - \hat{\psi}_m\hat{\omega}_{n-m\overline{y}}\right] = 0. \tag{3.23}$$

This particular numerical scheme then proceeded by the use of second-order central finite differencing in $\overline{y}$, (implicit) Crank-Nicolson second-order differencing in $\overline{X}$, together with truncation of the series (3.20), (3.21) at $n = \pm N$. The boundary conditions appropriate to this system are that all $\hat{\psi}_n$ are bounded as $\overline{y} \to \infty$ and

$$\hat{\psi}_n(\overline{y}=0) = 0 \quad \forall n. \tag{3.24}$$

Taking the convective gust problem (on which we focus most of our attention, although conceptually there is little difference in taking the more general class of free-stream disturbance), then we have that as $\overline{y} \to \infty$

$$\hat{\omega}_n \to 0 \quad \text{for} \quad n \neq \pm 1, \tag{3.25}$$

but

$$\hat{\omega}_{\pm 1} \to \omega_1^0. \tag{3.26}$$

Although this scheme did provide accurate solutions at small and moderate values of $\overline{X}$, after some investigation it was found that at larger values of $\overline{X}$, the truncation errors associated with this scheme became increasingly large, and substantially larger values of the parameter N were required in order to maintain accuracy which in turn demanded the use of smaller values of the step size $\Delta\overline{X}$; correspondingly, substantially longer computing times were then necessary. In an attempt to resolve this difficulty, the scheme was modified to a pseudo-spectral scheme, in which the solution in spectral (n) space was fast-Fourier transformed into physical (ξ) space, in which the nonlinear

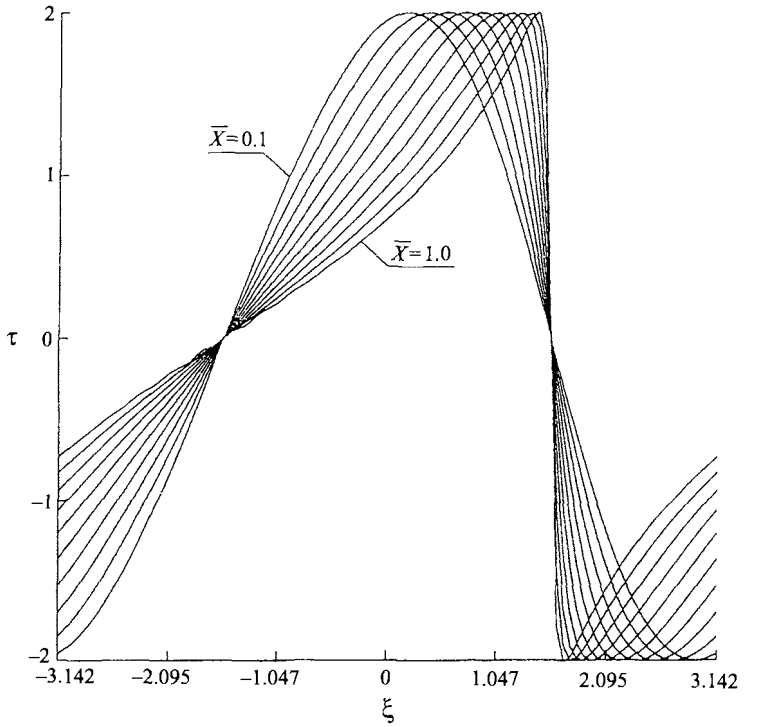

FIGURE 3. Wall vorticity distributions ($\tau = \omega_1(\bar{y} = 0)$) for $\alpha = 1, \beta = 0$.

(convolution) terms were evaluated, and then fast-Fourier transformed back into spectral (n) space. However this scheme was susceptible to aliasing errors, which were difficult to control.

As an alternative to the above procedures, the solution was also carried out using a fully second-order finite-difference scheme. In order to improve accuracy, two coordinate mappings were implemented, one of the form $\xi = f(\zeta)$, the other of the form $\bar{y} = g(\eta)$. The problem in terms of η and ζ may then be stated in the form

$$\frac{1}{f'^2(\zeta)}\psi_{1\zeta\zeta} - \frac{f''(\zeta)}{f'^3(\zeta)}\psi_{1\zeta} + \frac{1}{g'^2(\eta)}\psi_{1\eta\eta} - \frac{g''(\eta)}{g'^3(\eta)}\psi_{1\eta} = -\omega_1, \tag{3.27}$$

together with

$$f'(\zeta)g'(\eta)\frac{\partial\omega_1}{\partial\bar{X}} + \psi_{1\eta}\omega_{1\zeta} - \psi_{1\zeta}\omega_{1\eta} = 0, \tag{3.28}$$

with appropriate (periodic) boundary conditions in ζ. This technique then allowed 'bunching' of grid points close to $\bar{y} = \eta = 0$ and also close to some specified $\zeta(\xi)$ location, once a finite-difference approximation had been made.

In the case of the spectral method, typically we took $N = 120$, with a transverse grid that extended to $\bar{y} = 10$, with 301 grid points, and a 'time' step of $\Delta\bar{X} = 0.005$. For the fully finite-difference scheme, we generally took 641 points in ζ, 321 points in η, with a grid that extended out to $\bar{y} \approx 20$ in the physical coordinate, with $\Delta\bar{X} = 0.005$. We carried out detailed computations for two sets of data. The first corresponds to $\alpha = 1$, $\beta = 0$. Results for the wall vorticity (shear) distribution with ξ at selected values of $\bar{X}$ are shown in figure 3. Note that for these data, there exists symmetry/antisymmetry about $\xi = \pm\pi/2$, a feature of the solution that our finite-difference scheme was able

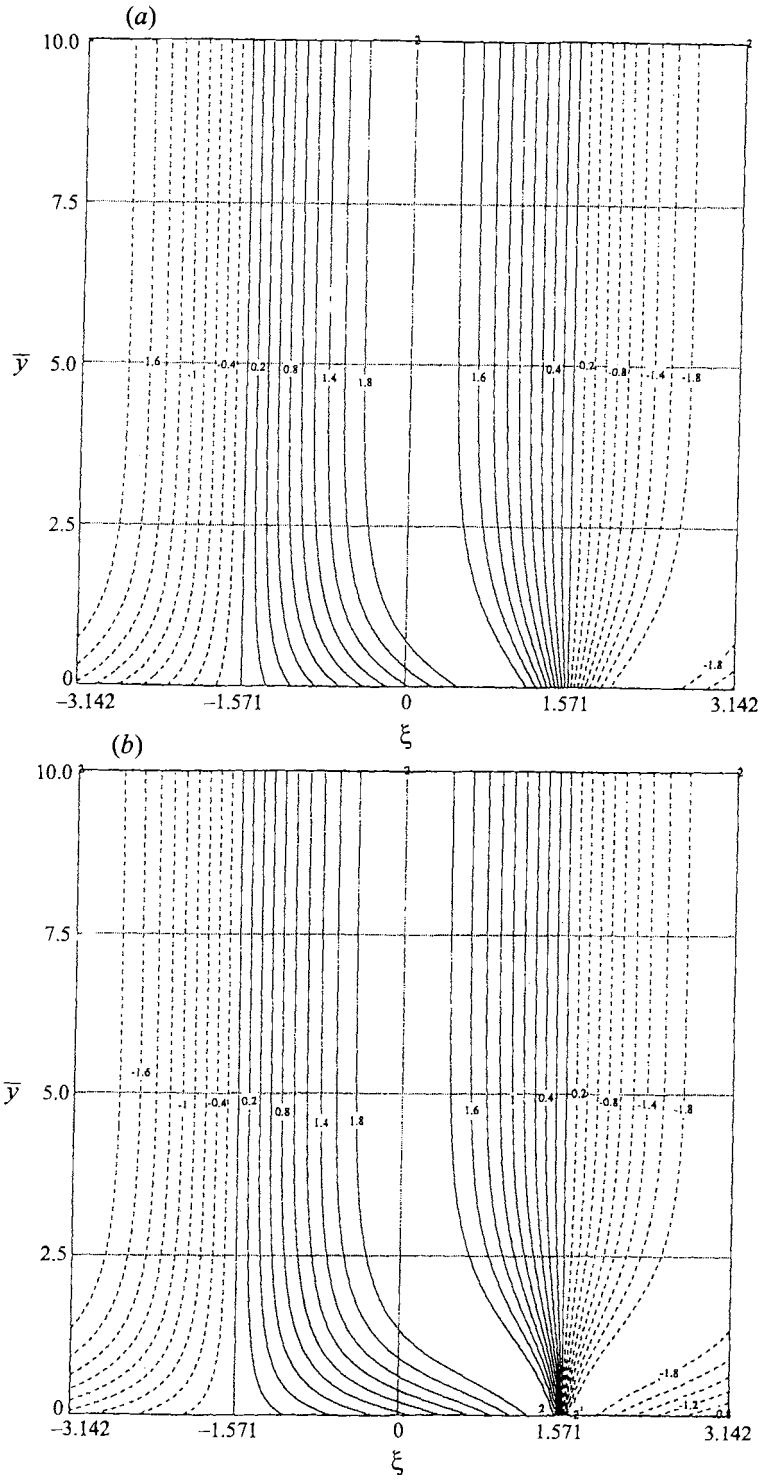

FIGURE 4 (*a*, *b*). For caption see facing page.

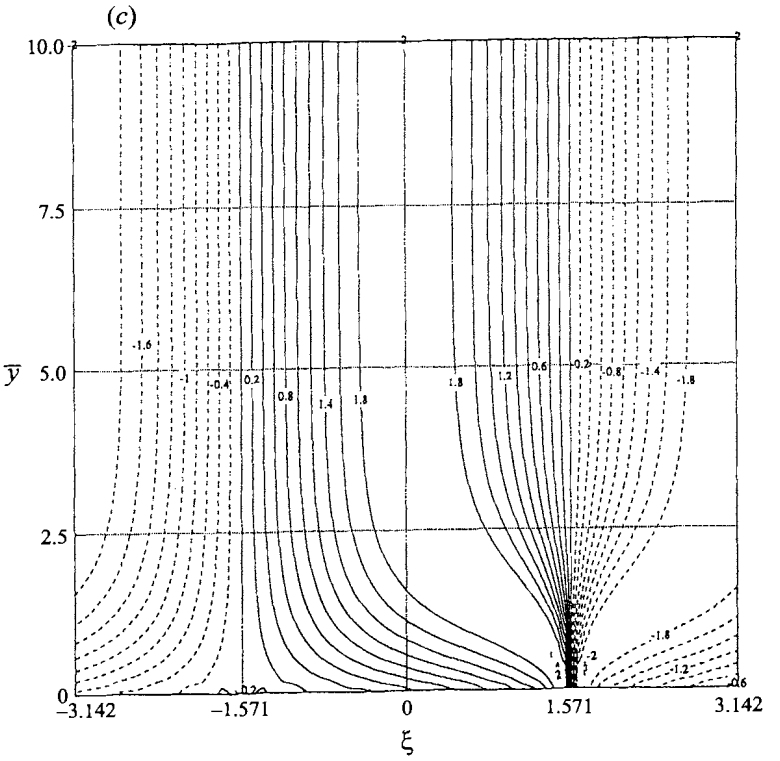

FIGURE 4. Vorticity contours for $\alpha = 1, \beta = 0$: (*a*) $\overline{X} = 0.5$, (*b*) $\overline{X} = 1.0$, (*c*) $\overline{X} = 1.25$.

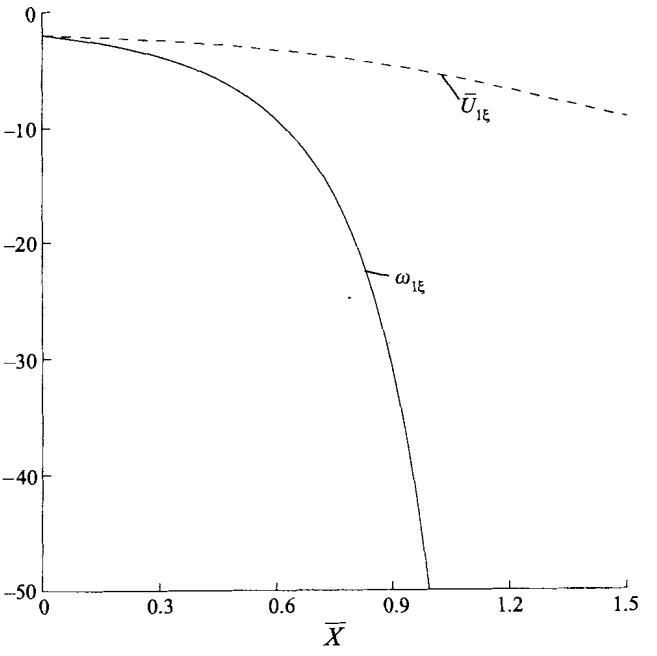

FIGURE 5. Variation of $\partial\omega_1/\partial\xi(\xi = \frac{1}{2}\pi, \bar{y} = 0)$ and $\partial\overline{U}_1/\partial\xi(\xi = \frac{1}{2}\pi, \bar{y} = 0)$ with $\overline{X}$ for $\alpha = 1, \beta = 0$.

to exploit, by halving the computational domain. Figure 3 reveals very clearly the development of an increasing steepening of the wall-vorticity distribution, strongly pointing to the development of a shock-like distribution forming at some finite value of $\bar{X} = \bar{X}_s$, centred around the point $\xi = \xi_s = \pi/2$. Indeed, this point is significant, corresponding exactly to the point where the vorticity is zero (for all $\bar{X}$), which significantly in turn corresponds to effectively a stagnation point lying on the wall surface. Indeed, the maximum amplitude of the vorticity is always bounded (as it must be) whilst the vorticity at $\xi = \xi_s, \bar{y} = 0$ must always remain zero on account of the antisymmetry about this point, which in turn leads to the fact that ξ_s remains a stagnation point.

Figure (4*a–c*) shows contours of constant vorticity throughout the flow-field, at selected values of $\bar{X}$. These reveal a 'pinching' of the vorticity contours close to $\xi = \pi/2$, as the critical value of $\bar{X}$ is approached. Figure 5 shows the development of $\partial\omega_1/\partial\xi(\xi = \pi/2, \bar{y} = 0)$ and $\partial\bar{U}_1/\partial\xi(\xi = \pi/2, \bar{y} = 0)$ with $\bar{X}$. These results reinforce the concept of the development of a short lengthscale around $\xi = \pi/2$; it does appear that the singularity in the vorticity distribution is considerably stronger than in the streamwise velocity distribution. This point is important in developing an analytic description of the singular behaviour of the flow.

The second case considered was $\alpha = \beta = 1$. Results for the wall vorticity distribution are shown in figure 6. In this case the symmetry arguments are no longer appropriate. From these results, it is again clear that a shock-like structure in the wall vorticity is developing, this time close to $\xi = \xi_s = \pi/4$, at which point again, the vorticity remains constant for all $\bar{X}$, although in this case the vorticity is non-zero there; however this point does correspond to a stagnation point of the flow field. Note that in the general case stagnation points occur at $\xi = 1/\alpha \arctan(\alpha/\beta)$. This arises because on $\bar{y} = 0$, $\bar{V}_1 = -\psi_{1\xi} = 0$ for all $\bar{X}$, whilst $\bar{U}_1(\bar{y} = 0, \bar{X} = 0) = \psi_{1\bar{y}}(\bar{y} = 0, \bar{X} = 0) = 0$ provided $\xi = 1/\alpha \arctan(\alpha/\beta)$ (see (3.15)). However by (3.10) we then see that $\partial\omega_1/\partial\bar{X}(\bar{y} = 0, \bar{X} = 0) = 0$ at this point, and so ω_1 remains initially unchanged at this point. However the additional constraint of periodicity in ξ leads to the conclusion that $\partial\omega_1/\partial\bar{X} = \bar{U}_1 = \bar{V}_1 = 0$ at this point for all $\bar{X}$. This conclusion is confirmed at the second order in $\bar{X}$, as shown by (3.16); consequently all effective stagnation points remain effective stagnation points, and the value of the vorticity, ω_1, at these points remains constant. Figure 7*a–c* shows the lines of constant vorticity throughout the flow field, and again the pinching behaviour close to $\xi = \xi_s$ is seen to develop as $\bar{X}$ increases. The development of $\omega_{1\xi}(\xi = \xi_s, \bar{y} = 0)$ and $u_{1\xi}(\xi = \xi_s, \bar{y} = 0)$ are shown in figure 8.

The nature of this singularity is of great interest. It is very clear from our numerical results that (i) a small streamwise scale emerges close to the singular point ξ_s when $\bar{X}$ approaches the critical value $\bar{X}_s$; (ii) the vorticity ω_1 remains bounded; (iii) the strength of the singularity of the derivative of the wall vorticity is substantially greater than that of the streamwise velocity; and (iv) the singularity occurs at the stagnation point located on the wall. Guided by the above, one plausible structure is as follows. We write

$$\hat{\xi} = \frac{\xi - \xi_s}{\tau^\gamma}, \tag{3.29}$$

where $\tau = \bar{X}_s - \bar{X}$ and γ is an index which is to be determined. It would appear that the only sensible rational solution development takes the form

$$\psi_1 = \tau^{2\gamma-2}\hat{\xi} \int_0^{\hat{y}} \hat{u}(\hat{y})\mathrm{d}\hat{y} + \tau^{2\gamma}\hat{\psi}_1(\hat{\xi}, \hat{y}) + \ldots, \tag{3.30}$$

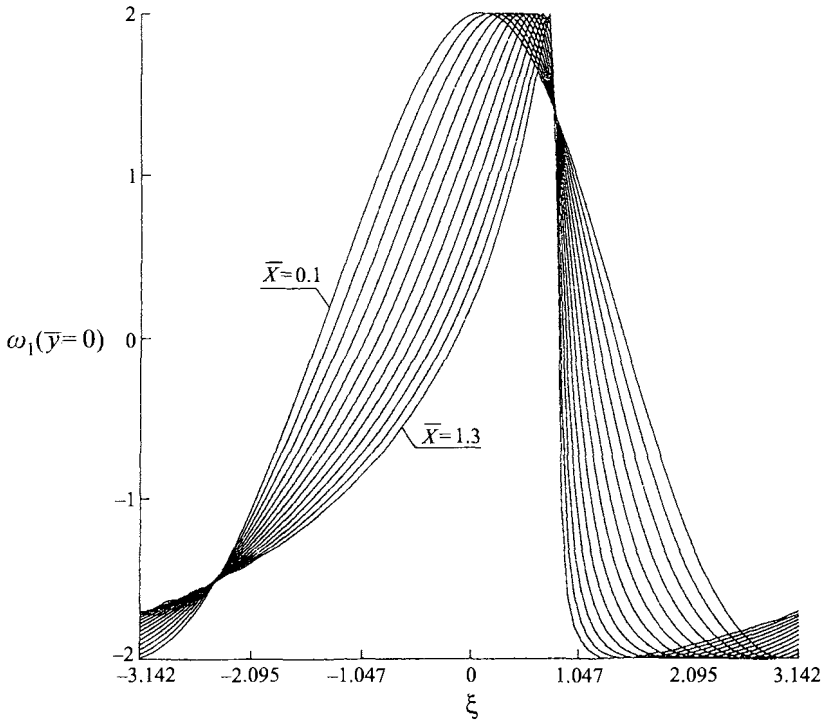

FIGURE 6. Wall vorticity distributions for $\alpha = 1, \beta = 1$.

where $\hat{y} = \bar{y}/\tau^{\gamma-1}$, and

$$\omega_1 = \omega_{10} + \hat{\xi}\hat{u}_{\hat{y}} + \hat{\psi}_{1\hat{\xi}\hat{\xi}} + \ldots \tag{3.31}$$

(where $\omega_{10} = 2\omega_1^0 \cos(\alpha\xi_s)$ is a constant) which leads to the system

$$\gamma\hat{\xi}(\hat{u}_{\hat{y}}+\hat{\psi}_{1\hat{\xi}\hat{\xi}\hat{\xi}})+(\gamma-1)\hat{y}(\hat{\xi}\hat{u}_{\hat{y}\hat{y}}+\hat{\psi}_{1\hat{y}\hat{\xi}\hat{\xi}})+\hat{\xi}\hat{u}(\hat{u}_{\hat{y}}+\hat{\psi}_{1\hat{\xi}\hat{\xi}\hat{\xi}})-\int_0^{\hat{y}}\hat{u}\mathrm{d}\hat{y}(\hat{\xi}\hat{u}_{\hat{y}\hat{y}}+\hat{\psi}_{1\hat{\xi}\hat{\xi}\hat{y}}) = 0. \tag{3.32}$$

Implementation of the $\hat{y} = 0$ boundary condition leads to the result that $\hat{u}|_{\hat{y}=0} = -\gamma$, whilst as $|\xi| \to \infty$,

$$\hat{\psi}_{1\hat{\xi}\hat{\xi}} \to -\hat{\xi}\hat{u}_{\hat{y}}. \tag{3.33}$$

The determination of γ must be obtained from the solution to the full system (3.27)–(3.28); our numerical solution, although unable to accurately determine the numerical value of γ because of numerical difficulties, does indicate values in excess of '4' in the case of $\alpha = 1$, and $\beta = 0$. Indeed, the relative largeness of this value is to a large extent responsible for the difficulty in its accurate determination, because of the corresponding large solution gradients, which in turn lead to a large numerical dissipation, which obviously becomes compounded as the location of the breakdown is approached. Indeed there are a number of similarities here with the difficulties associated with the numerical solution of Burgers' equation, which has some obvious similarities in form with our system.

We now consider the effects of a wall roughness element located upstream of the singular point, i.e. $\bar{X} = \epsilon Re^{1/4}$ at the roughness location is smaller than $\bar{X}_s$ then

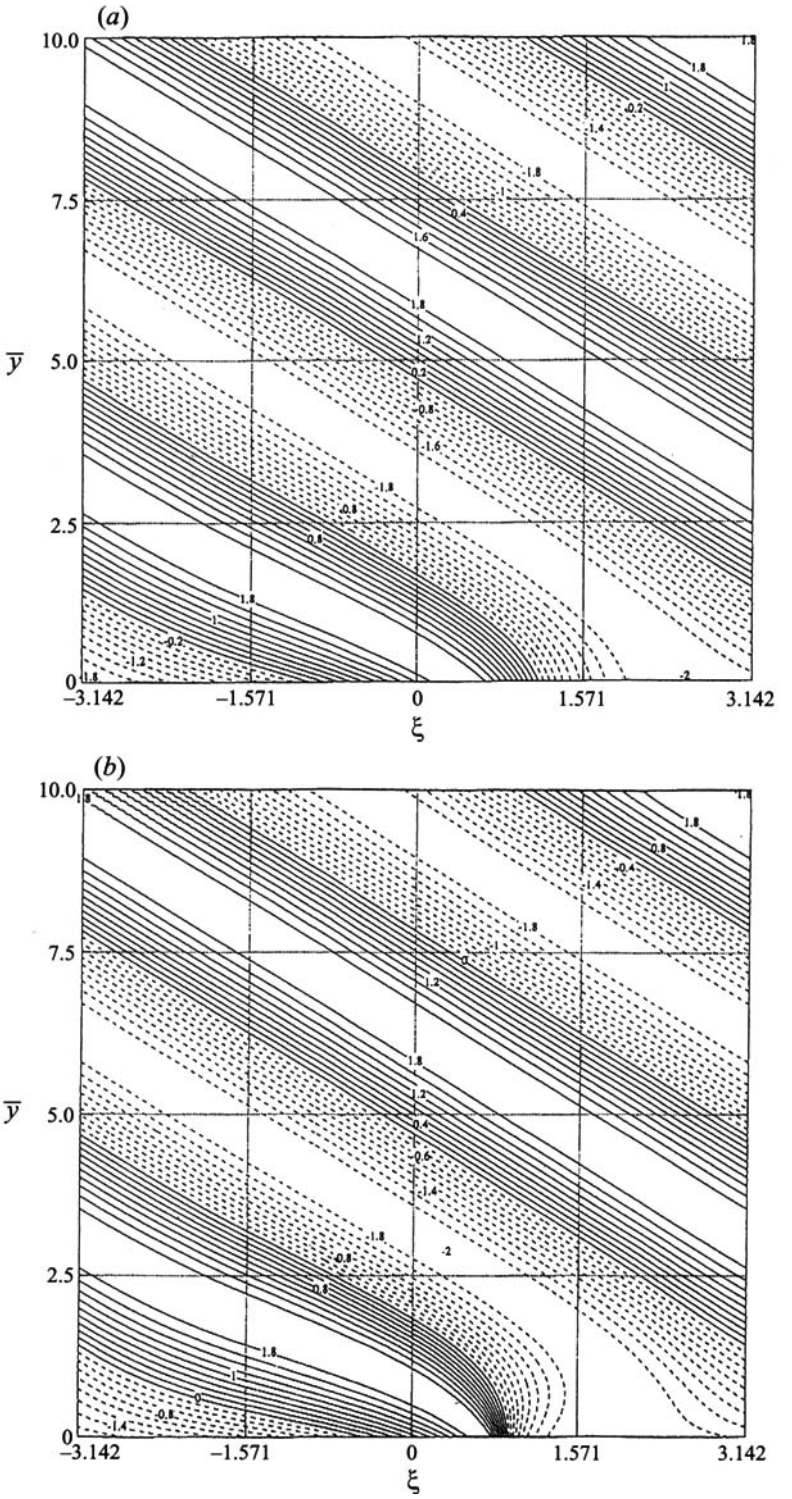

FIGURE 7 (*a*, *b*). For caption see facing page.

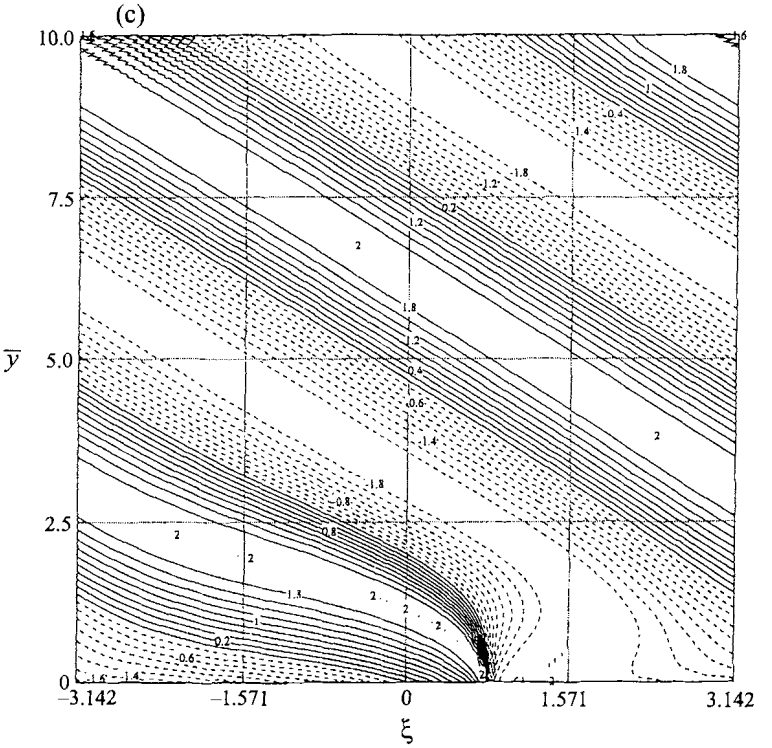

FIGURE 7. Vorticity contours for $\alpha = 1, \beta = 1$: (*a*) $\overline{X} = 0.5$, (*b*) $\overline{X} = 1.0$, (*c*) $\overline{X} = 1.5$.

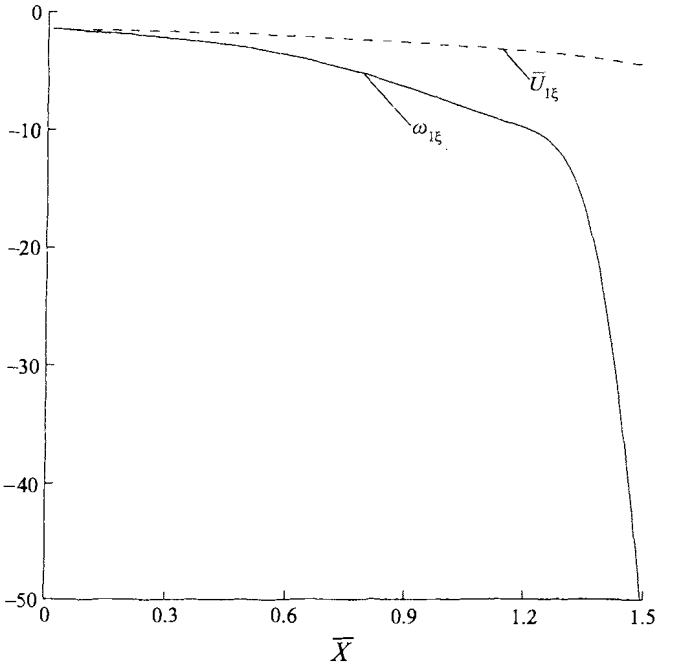

FIGURE 8. Variation of $\partial\omega_1/\partial\xi(\xi = \frac{1}{2}\pi, \bar{y} = 0)$ and $\partial\overline{U}_1/\partial\xi(\xi = \frac{1}{2}\pi, \bar{y} = 0)$ with $\overline{X}$ for $\alpha = 1, \beta = 1$.

the analysis of the Tollmien–Schlichting waves generation process is appropriate. This requires a knowledge of the velocity and the pressure fields near the roughness element. In the vortex layer (region 1 in figure 2) these take the form

$$\left.\begin{aligned} u &= 1 + \epsilon\overline{U}_1(\xi,\overline{X},\overline{y}) + \epsilon^2\overline{U}_2(\xi,\overline{X},\overline{y}) + \ldots, \\ v &= \epsilon\overline{V}_1(\xi,\overline{X},\overline{y}) + \epsilon^2\overline{V}_2(\xi,\overline{X},\overline{y}) + \ldots, \\ p &= \epsilon^2\overline{P}_2(\xi,\overline{X},\overline{y}) + \ldots \end{aligned}\right\} \tag{3.34}$$

All the terms $\overline{U}_1, \overline{U}_2, \overline{V}_1, \overline{V}_2, \overline{P}_2$, etc. in the asymptotic expansions (3.34) are periodic functions of ξ. For example, the pressure near the bottom of the vortex layer may be expressed in Fourier series form

$$\overline{P}_2(\xi,\overline{X},0) = \sum_{n=-\infty}^{\infty} P_n(\overline{X})\mathrm{e}^{in\alpha\xi}. \tag{3.35}$$

Similarly, we can write

$$\overline{U}_1(\xi,\overline{X},0) = \sum_{n=-\infty}^{\infty} \overline{U}_{1n}(\overline{X})\mathrm{e}^{in\alpha\xi}, \tag{3.36}$$

where

$$P_{-n} = \text{c.c.}P_n, \qquad \overline{U}_{1(-n)} = \text{c.c.}\overline{U}_{1n},$$

The stationary boundary-layer flow upstream of the roughness may be described by the Blasius solution

$$u = U_b(x,Y) + \ldots, \qquad v = Re^{-1/2}V_b(x,Y) + \ldots,$$

where $Y = Re^{1/2}y$ and

$$U_b = f'(\eta), \quad V_b = -\tfrac{1}{2}x^{-1/2}(f - \eta f'), \quad \eta = Re^{-1/2}\frac{y}{x^{1/2}}, \tag{3.37}$$

with the function $f(\eta)$ representing the solution to the Blasius equation

$$f''' + \tfrac{1}{2}ff'' = 0, \quad f(0) = f'(0) = 0, \quad f(\infty) = 1.$$

It follows from the matching condition with the solution (3.34)–(3.36) in the vortex layer that the non-stationary flow in the boundary layer takes the following asymptotic form:

$$\left.\begin{aligned} u &= U_b(x,Y) + \epsilon U_1(\xi,x,\overline{X},Y) + \ldots, \\ v &= Re^{-1/2}V_b(x,Y) + \epsilon Re^{-1/4}V_1(\xi,x,\overline{X},Y) + \ldots, \\ p &= \epsilon^2 P_2(\xi,\overline{X},Y) + \ldots. \end{aligned}\right\} \tag{3.38}$$

Substitution of (3.38) into the Navier–Stokes equations (2.1) leads to

$$(U_b - 1)\frac{\partial U_1}{\partial\xi} + V_1\frac{\partial U_b}{\partial Y} = 0, \qquad \frac{\partial U_1}{\partial\xi} + \frac{\partial V_1}{\partial Y} = 0, \tag{3.39}$$

or by eliminating $\partial U_1/\partial\xi$

$$(U_b - 1)\frac{\partial V_1}{\partial Y} - V_1\frac{\partial U_b}{\partial Y} = 0,$$

which is equivalent to

$$\frac{\partial}{\partial Y}\left(\frac{V_1}{U_b - 1}\right) = 0.$$

This equation may be integrated, and with the impermeability condition at the wall namely $V_1 = 0$ at $Y = 0$, leads to the conclusion that V_1 is identically zero in the boundary layer. Further, it easily follows from (3.39) that $\partial U_1/\partial\xi$ must also be zero and so no oscillatory term of $O(\epsilon)$ may exist in the asymptotic expansion (3.38) for the longitudinal velocity component u in the boundary layer.

In order to smooth out this jump in the $O(\epsilon)$ longitudinal velocity oscillations in the outer vortex flow, which are not present inside the boundary layer, an intermediate shear layer (region 2′ in figure 2) must be introduced near the outer edge of the boundary layer. If the $O(\epsilon^2)$ terms are included in the asymptotic expansions (3.38) for u and v, then the boundary layer by itself divides into two parts, region 2 and region 3 (see figure 2). Region 2 is the bulk of the boundary layer where the flow appears to be effectively inviscid with respect to high-frequency oscillations. Region 3 is a thin viscous Stokes layer which serves to satisfy the no-slip condition on the surface.

Consider first the intermediate viscous layer 2′. Here a new normal variable $\hat{y}$ is introduced as follows (see Guliaev *et al.* 1989)

$$y = Re^{-1/2}\,[Y_0(x, Re) + \delta(x, Re)\hat{y}]\,, \tag{3.40}$$

where the 'centreline' Y_0 and intermediate layer thickness δ are to be determined. As the intermediate layer is located near the outer edge of the boundary layer and viscous forces must be significant, it is reasonable to expect that $Y_0 \to \infty$ and $\delta \to 0$ as $Re \to \infty$.

The velocity components in region 2′ may be written in the form

$$\left.\begin{aligned} u &= U_b + \epsilon\hat{U}_1(\xi, x, \overline{X}, \hat{y}) + \ldots, \\ v &= Re^{-1/2}V_b + \epsilon\delta Re^{-1/4}\hat{V}_1(\xi, x, \overline{X}, \hat{y}) + \ldots, \end{aligned}\right\} \tag{3.41}$$

where the leading-order terms U_b and V_b again represent the Blasius stationary solution (3.37). It is known that near the outer edge of the boundary layer

$$U_b = 1 - \frac{A}{\eta - \eta_1}\exp\left[-\frac{(\eta - \eta_1)^2}{4}\right] + \ldots, \tag{3.42}$$

with $A \approx 0.46$ and $\eta_1 \approx 1.72$, and η is defined below.

In order to determine Y_0 and δ in (3.40), a balance of longitudinal and transverse inertial terms with the viscous term in the longitudinal momentum equation (2.1) has to be considered, i.e.

$$\epsilon Re^{1/4}(U_b - 1)\frac{\partial\hat{U}_1}{\partial x} \sim \epsilon\delta Re^{1/4}\frac{1}{x^{1/2}}\hat{V}_1\frac{\mathrm{d}U_b}{\mathrm{d}\eta} \sim \frac{\epsilon}{\delta^2}\frac{\partial^2\hat{U}_1}{\partial\hat{y}^2}. \tag{3.43}$$

Taking into account the asymptotic behaviour of U_b as indicated in (3.42), and taking

$$\eta = \frac{Y_0 + \delta\hat{y}}{x^{1/2}},$$

it can be easily shown that (see Guliaev *et al.* 1989)

$$Y_0(x, Re) = \eta_0(Re)x^{1/2}, \qquad \delta(Re) = \frac{2}{\eta_0(Re)},$$

with η_0 satisfying the transcendental equation

$$\eta_0^3 e^{\eta_0^2/4} = 4ARe^{1/4},$$

and so

$$\eta_0^2 = \tfrac{1}{4}\log Re - \tfrac{3}{2}\log\log Re + \ldots \quad \text{as} \quad Re \to \infty.$$

It should be noted here that the nonlinear terms in the longitudinal momentum equation are $O(\epsilon^2 Re^{1/4})$, and so comparing linear and nonlinear terms, it can be shown the condition (3.43) that controls the location and thickness of the intermediate layer is valid provided

$$\epsilon \ll \eta_0^2 Re^{-1/4}. \tag{3.44}$$

If $\epsilon \geqslant O(\eta_0^2 Re^{-1/4})$, the resultant problem for the intermediate layer is nonlinear in general and so requires a more complicated analysis. Since our purpose is to verify the principal possibility for Tollmien–Schlichting waves to be generated by free-stream turbulence, in the subsequent analysis we have assumed that in sublayer 2′ the perturbation amplitude is small enough to satisfy (3.44). Hence, the problem for region 2′ may be reduced to

$$\left.\begin{aligned} -e^{-\hat{y}/x^{1/2}}\frac{\partial \hat{U}_1}{\partial \xi} - \frac{1}{x^{1/2}}\frac{\partial \hat{U}_1}{\partial \hat{y}} + \frac{1}{x^{1/2}}e^{-\hat{y}/x^{1/2}}\hat{V}_1 &= \frac{\partial^2 \hat{U}_1}{\partial \hat{y}^2}, \\ \frac{\partial \hat{U}_1}{\partial \xi} + \frac{\partial \hat{V}_1}{\partial \hat{y}} &= 0. \end{aligned}\right\} \tag{3.45}$$

Since equations (3.45) are linear, it is convenient to seek solutions in the form of Fourier series

$$\hat{U}_1 = \sum_{n=-\infty}^{\infty} \hat{U}_{1n}(x, \overline{X}, \hat{y})e^{in\alpha\xi}, \quad \hat{V}_1 = \sum_{n=-\infty}^{\infty} \hat{V}_{1n}(x, \overline{X}, \hat{y})e^{in\alpha\xi}. \tag{3.46}$$

Each Fourier mode may then be treated independently, and so from (3.45), (3.46)

$$\frac{\partial^3 \hat{V}_{1n}}{\partial \hat{y}^3} + \frac{1}{x^{1/2}}\frac{\partial^2 \hat{V}_{1n}}{\partial \hat{y}^2} + in\alpha e^{-\hat{y}/x^{1/2}}\left(\frac{\partial \hat{V}_{1n}}{\partial \hat{y}} + \frac{1}{x^{1/2}}\hat{V}_{1n}\right) = 0. \tag{3.47}$$

Without loss of generality we may assume $\alpha > 0$. The boundary conditions for (3.47) arise from matching with the solution in the bulk of the boundary layer (region 2 in figure 2)

$$\hat{V}_{1n} \to 0 \quad \text{as} \quad \hat{y} \to -\infty, \tag{3.48}$$

and also matching with the solution represented by (3.34), (3.36) in the vortex layer (region 1)

$$\frac{\partial \hat{V}_{1n}}{\partial \hat{y}} \to -in\alpha \overline{U}_{1n}(\overline{X}) \quad \text{as} \quad \hat{y} \to +\infty. \tag{3.49}$$

Introducing the new independent variable

$$z = 2(i\alpha n x)e^{-\hat{y}/(2x^{1/2})},$$

the solution for (3.47)–(3.49) may be expressed in terms of Hankel functions $H_0^{(1)}$ and $H_0^{(2)}$:

$$\hat{V}_{1n}(z) = 2\pi n\alpha x^{1/2}\overline{U}_{1n}(\overline{X})z^2 \int_z^{\infty} z^{-3}H_0^{(1)}(z)\mathrm{d}z \quad \text{for} \quad n > 0, \tag{3.50}$$

$$\hat{V}_{1n}(z) = 0 \quad \text{for} \quad n = 0, \tag{3.51}$$

$$\hat{V}_{1n}(z) = -2\pi n\alpha x^{1/2}\overline{U}_{1n}(\overline{X})z^2 \int_z^{\infty} z^{-3}H_0^{(2)}(z)\mathrm{d}z \quad \text{for} \quad n < 0. \tag{3.52}$$

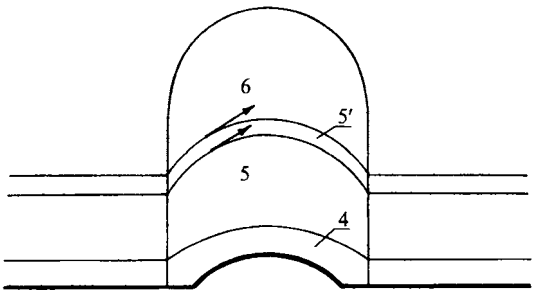

FIGURE 9. Triple-deck structure.

Using the asymptotic behaviour of Hankel functions as $z \to \infty$ along $\arg(z) = \pi/4$ for $n > 0$ (or along $\arg(z) = -\pi/4$ for $n < 0$) it can be shown that unsteady perturbations of $O(\epsilon)$ do not penetrate into the main part of the boundary layer, but rather exhibit a rapid exponential decay within the intermediate layer, as $\hat{y} \to -\infty$. Similar behaviour of pulsatory shear layers was shown to exist by Smith, Doorly & Rothmayer (1990) under quite different circumstances.

To formulate the boundary value problem for the triple-deck region in the vicinity of the roughness, we need to know the solution in the Stokes layer. This may be expressed in the form of the asymptotic expansions

$$\left.\begin{aligned} u &= Re^{-1/8}\tilde{U}_0(x, Y_*) + \epsilon^2\tilde{U}_2(\xi, \overline{X}, Y_*) + \ldots, \\ v &= Re^{-3/8}\tilde{V}_0(x, Y_*) + \epsilon^2 Re^{-3/8}\tilde{V}_2(\xi, \overline{X}, Y_*) + \ldots, \\ p &= \epsilon^2\overline{P}_2(\xi, \overline{X}, 0) + \ldots, \end{aligned}\right\} \tag{3.53}$$

with the transverse variable

$$Y_* = Re^{5/8}y. \tag{3.54}$$

Substitution of (3.53) into the Navier–Stokes equations (2.1) shows that

$$\tilde{U}_0(x, Y_*) = \lambda(x)Y_*, \tag{3.55}$$

where $\lambda(x)$ is the skin friction distribution along the flat plate in Blasius flow.

The oscillatory term $\tilde{U}_2$ in the longitudinal velocity component (3.53) may be shown to be

$$\tilde{U}_2 = \sum_{n=-\infty}^{\infty} P_n(\overline{X})\left\{1 - \exp\left[-\left(\tfrac{1}{2}n\alpha\right)^{1/2}(1-\mathrm{i})Y_*\right]\right\}\mathrm{e}^{\mathrm{i}n\alpha\xi}, \tag{3.56}$$

where the $P_n(\overline{X})$ are defined in (3.35).

4. Flow around the roughness

As mentioned in §1, the flow in the vicinity of the roughness has a triple-deck structure. This consists of a viscous near-wall layer (region 4 in figure 9), wherein $y = O(Re^{-5/8})$, the bulk of the boundary layer (region 5) with thickness $y = O(Re^{-1/2})$ and the external region 6, where $y = O(Re^{-3/8})$. The generation of Tollmien–Schlichting waves may result from the nonlinear interactions of the stationary flow perturbations around the roughness with the oscillating flow arising from the vorticity wave outside the boundary layer (in region 1 in figure 2) and boundary-layer oscillations, especially in the Stokes layer (region 3), upstream of the roughness. Under normal circumstances,

nonlinear effects are important only in the near-wall region 4, but the vorticity wave provokes very small oscillations in the Stokes layer compared with the oscillations outside the boundary layer. Consequently, as far as the Tollmien–Schlichting wave generation process is concerned, the role of nonlinear processes in region 6 may be more important than their role in the viscous sublayer 4.

The criterion may be ascertained in the following way. The pressure gradient in the vorticity wave leading to the flow oscillations in the Stokes layer may be estimated as

$$\frac{\partial p}{\partial x} = O\left(\frac{\epsilon^2}{Re^{-1/4}}\right). \tag{4.1}$$

On the other hand, an oscillating pressure gradient is also generated locally in the upper deck (region 6) owing to superposition of the stationary perturbations which are such that

$$u = O(Re^{-1/4}), \tag{4.2}$$

whilst the perturbations in the vorticity wave (in accordance with the solution represented by (3.34)) are such that

$$u = O(\epsilon). \tag{4.3}$$

The pressure perturbations may be estimated from the product of (4.2) and (4.3), and so

$$p = O(\epsilon Re^{-1/4}).$$

Since the characteristic longitudinal scale of the stationary velocity perturbations (4.2) is $\Delta x \sim Re^{-3/8}$, the pressure gradient

$$\frac{\partial p}{\partial x} = O\left(\frac{\epsilon Re^{-1/4}}{Re^{-3/8}}\right). \tag{4.4}$$

Comparison of (4.1) and (4.4) shows that there is a critical value of the amplitude

$$\epsilon^{**} = Re^{-1/8}.$$

If the amplitude ϵ of the vorticity oscillations in the free stream is small compared with ϵ^{**}, then the contribution of the upper deck in the Tollmien–Schlichting wave generation process is more important than the contribution of the viscous sublayer. If ϵ is greater than ϵ^{**}, then nonlinear effects in the viscous sublayer are dominant.

Since the wall roughness is taken to be upstream of the singularity in the vortex layer flow, i.e. $\bar{X} = \epsilon Re^{1/4} < \bar{X}_s$, in what follows the amplitude of free-stream perturbations ϵ is taken to be $O(Re^{-1/4})$ or less. In this case the condition (3.44) is satisfied automatically and ϵ appears to be much smaller than ϵ^{**}. Consequently the nonlinear interaction of the triple-deck flow with the near-wall Stokes layer (region 3 in figure 2) takes no part in the Tollmien–Schlichting wave generation process.

Consider the flow in the viscous near-wall layer (region 4), where

$$y = Re^{-5/8}Y_*, \qquad t = Re^{-1/4}\tilde{t}, \qquad x = 1 + Re^{-3/8}x_*. \tag{4.5}$$

The velocity components and the pressure have expansions

$$\left.\begin{aligned} u &= Re^{-1/8}U_0^* + Re^{-1/4}U_{01}^* + Re^{-3/8}U_{02}^* + \epsilon Re^{-1/8}U_1^* + \ldots, \\ v &= Re^{-3/8}V_0^* + Re^{-1/2}V_{01}^* + Re^{-5/8}V_{02}^* + \epsilon Re^{-3/8}V_1^* + \ldots, \\ p &= Re^{-1/4}P_0^* + Re^{-3/8}P_{01}^* + Re^{-1/2}P_{02}^* + \epsilon Re^{-1/4}P_1^* + \ldots. \end{aligned}\right\} \tag{4.6}$$

Here the first three terms represent stationary flow over the roughness, and therefore

U_{0i}^*, V_{0i}^* and P_{0i}^* with $i = 0, 1, 2$ depend on x_*, Y_* only. The fourth terms U_1^*, V_1^* and P_1^* describe non-stationary perturbations and depend on $\bar{t}, x_*, Y_*$. In the subsequent analysis only the leading-order stationary terms U_0^*, V_0^*, P_0^* and the first unsteady perturbations U_1^*, V_1^*, P_1^* are of significance as their interaction can produce Tollmien–Schlichting waves. Upon substituting (4.5), (4.6) into the Navier–Stokes equations (2.1) the following equations are obtained:

$$\left.\begin{aligned} U_0^*\frac{\partial U_0^*}{\partial x_*} + V_0^*\frac{\partial U_0^*}{\partial Y_*} &= -\frac{\partial P_0^*}{\partial x_*} + \frac{\partial^2 U_0^*}{\partial Y_*^2}, \\ \frac{\partial P_0^*}{\partial Y_*} = 0, \quad \frac{\partial U_0^*}{\partial x_*} &+ \frac{\partial V_0^*}{\partial Y_*} = 0, \end{aligned}\right\} \tag{4.7}$$

and

$$\left.\begin{aligned} \frac{\partial U_1^*}{\partial \bar{t}} + U_0^*\frac{\partial U_1^*}{\partial x_*} + U_1^*\frac{\partial U_0^*}{\partial x_*} + V_0^*\frac{\partial U_1^*}{\partial Y_*} + V_1^*\frac{\partial U_0^*}{\partial Y_*} &= -\frac{\partial P_1^*}{\partial x_*} + \frac{\partial^2 U_1^*}{\partial Y_*^2}, \\ \frac{\partial P_1^*}{\partial Y_*} = 0, \quad \frac{\partial U_1^*}{\partial x_*} &+ \frac{\partial V_1^*}{\partial Y_*} = 0. \end{aligned}\right\} \tag{4.8}$$

These equations must be solved with the no-slip and impermeability boundary conditions on the rigid-body surface (2.9)

$$U_0^* = V_0^* = U_1^* = V_1^* = 0 \quad \text{at} \quad Y_* = F(x_*), \tag{4.9}$$

and matching with the solution (3.53)–(3.56) in the Stokes layer upstream of the roughness (region 3 in figure 2) leads to

$$U_0^* \to \lambda Y_*, \quad U_1^* \to 0 \quad \text{as} \quad x_* \to -\infty. \tag{4.10}$$

It is straightforward to show that near the outer edge of region 4, the solutions of (4.7), (4.8) may be expressed in the form

$$U_0^* = \lambda Y_* + A_0^*(x_*) + \ldots, \quad V_0^* = -Y_*\frac{\mathrm{d}A_0^*}{\mathrm{d}x_*} + \ldots,$$

$$U_1^* = A_1^*(\bar{t}, x_*) + \ldots, \quad V_1^* = -Y^*\frac{\partial A_1^*}{\partial x_*} + \ldots, \tag{4.11}$$

as $Y_* \to \infty$.

Functions A_0^* and A_1^* are displacement functions, and represent the displacement effect of the boundary layer on the external flow. These functions, as well as the pressure gradients $\partial P_0^*/\partial x_*$ and $\partial P_1^*/\partial x_*$ in (4.7), (4.8) are unknown *a priori* .

In order to match with the viscous sublayer solution (4.6), (4.11) the solution in the bulk of the boundary layer (region 5 in figure 9) where $y = Re^{-1/2}Y$ must be expanded in the form

$$\left.\begin{aligned} u &= U_b(Y) + Re^{-1/8}U^0(x_*, Y) + \ldots + \epsilon Re^{-1/8}U^1(\bar{t}, x_*, Y) + \ldots, \\ v &= Re^{-1/4}V^0(x_*, Y) + \ldots + \epsilon Re^{-1/4}V^1(\bar{t}, x_*, Y) + \ldots, \\ p &= Re^{-1/4}P^0(x_*, Y) + \ldots + \epsilon Re^{-1/4}P^1(\bar{t}, x_*, Y) + \ldots. \end{aligned}\right\} \tag{4.12}$$

In the expressions above, $U_b(Y)$ is the Blasius velocity profile at $x = 1$ and only the leading-order stationary terms and the leading-order unsteady terms are indicated, all others being omitted for brevity.

Upon substitution of (4.12) into (2.1) and matching with the solution (4.6), (4.11) in the viscous near-wall region 4, it is easily verified that

$$U^0 = \frac{1}{\lambda}A_0^*(x_*)U_b'(Y), \quad V^0 = -\frac{1}{\lambda}\frac{\mathrm{d}A_0^*}{\mathrm{d}x_*}U_b(Y), \quad P^0 = P_0^*(x_*), \tag{4.13}$$

and

$$U^1 = \frac{1}{\lambda}A_1^*(\bar{t}, x_*)U_b'(Y), \quad V^1 = -\frac{1}{\lambda}\frac{\partial A_1^*}{\partial x_*}U_b(Y), \quad P^1 = P_1^*(\bar{t}, x_*), \tag{4.14}$$

where P_0^* and P_1^* are the corresponding terms from the pressure expansion (4.6) in region 4 (see figure 9). These are independent of the normal variable Y_* in this region, while P^0 and P^1 do not vary transversely across region 5.

Consider now the external region 6 (figure 9), where $y = Re^{-3/8}y_*$. It follows from matching with solution represented by (3.34) for the turbulence deformation layer, that velocity components and pressure in region 6 must be sought in the form

$$\left.\begin{aligned} u &= 1 + Re^{-1/4}u_0^*(x_*, y_*) + \epsilon\overline{U}_1[\xi_0(\bar{t}), \overline{X}_0, 0] + \ldots + \epsilon Re^{-1/4}u_1^*(\bar{t}, x_*, y_*) + \ldots, \\ v &= Re^{-1/4}v_0^*(x_*, y_*) + \ldots + \epsilon Re^{-1/4}v_1^*(\bar{t}, x_*, y_*) + \ldots, \\ p &= Re^{-1/4}p_0^*(x_*, y_*) + \ldots + Re^{-3/8}p_1^*(\bar{t}, x_*, y_*) + \ldots. \end{aligned}\right\} \tag{4.15}$$

The leading-order term in the longitudinal velocity component expansion (4.15) corresponds to the uniform undisturbed flow outside the boundary layer, the $Re^{-1/4}u_0^*$ term represents stationary perturbations produced by the roughness, while the $\epsilon\overline{U}_1$ term represents flow oscillations in the vorticity wave just at the roughness location. This is a function of time only, with $\xi_0(\bar{t})$ being defined as

$$\xi_0(\bar{t}) = \bar{x}_0 - \bar{t},$$

and constants $\bar{x}_0, \overline{X}_0$ are then $\bar{x}$- and $\overline{X}$-coordinates of the roughness 'center'. Stationary flow over the roughness is described by u_0^*, v_0^*, p_0^*, while only the leading-order stationary terms have been included. The terms u_1^*, v_1^*, p_1^* appear in (4.15) as a result of nonlinear interactions between stationary perturbations and oscillatory fluctuations of the flow, and so their order of magnitude $\epsilon Re^{-1/4}$ is simply the product of the order of magnitude of the stationary perturbations ($Re^{-1/4}$) and the amplitude of the turbulent oscillations (ϵ).

Substitution of (4.15) into (2.1) gives

$$\frac{\partial u_0^*}{\partial x_*} = -\frac{\partial p_0^*}{\partial x_*}, \quad \frac{\partial v_0^*}{\partial x_*} = -\frac{\partial p_0^*}{\partial y_*}, \quad \frac{\partial u_0^*}{\partial x_*} + \frac{\partial v_0^*}{\partial y_*} = 0. \tag{4.16}$$

The boundary conditions for (4.16) are the usual conditions of disturbance attenuation far from the roughness:

$$(u_0^*, v_0^*, p_0^*) \to 0 \quad \text{as} \quad x_*^2 + y_*^2 \to \infty, \tag{4.17}$$

and the matching condition with the solution (4.13) in the bulk of the boundary layer leads to

$$v_0^* = -\frac{1}{\lambda}\frac{\mathrm{d}A_0^*}{\mathrm{d}x_*} \quad \text{at} \quad y_* = 0. \tag{4.18}$$

The oscillatory terms satisfy

$$\frac{\partial u_1^*}{\partial x_*} + \frac{\partial p_1^*}{\partial x_*} = -\overline{U}_1\frac{\partial u_0^*}{\partial x_*}, \quad \frac{\partial v_1^*}{\partial x_*} + \frac{\partial p_1^*}{\partial y_*} = -\overline{U}_1\frac{\partial v_0^*}{\partial x_*}, \quad \frac{\partial u_1^*}{\partial x_*} + \frac{\partial v_1^*}{\partial y_*} = 0. \tag{4.19}$$

The condition of attenuation is similar to (4.17), namely

$$(u_1^*, v_1^*, p_1^*) \to 0 \quad \text{as} \quad x_*^2 + y_*^2 \to \infty. \tag{4.20}$$

Equation (4.19) also requires a boundary condition on $y_* = 0$, similar to (4.18). The straightforward procedure to formulate the condition consists of matching of the expansion (4.15) with the solution in region 5′ (see figure 9), which represents the continuation of the intermediate layer 2′ (figure 2) into the triple-deck region. The solution in region 5′ in turn should be matched with the solution (4.12)-(4.14) in the bulk of the boundary layer (region 5 in figure 9). Meanwhile it is easily seen that there is no need to follow this lengthy procedure. One can simply take into account that the displacement thickness of the boundary layer in the triple-deck region is influenced only by the viscous near-wall sublayer 4, where the fluid velocity is small and the flow reveals high sensitivity to the pressure variation along streamlines. In the bulk of the boundary layer the fluid velocity is an order of magnitude greater than in the sublayer and so, in spite of its relatively large thickness, the bulk of the boundary layer (region 5) does not contribute to the displacement thickness of the boundary layer as a whole. In region 5′ the velocity is of the same order of magnitude as that in region 5, but the thickness is smaller. For this reason region 5′ will not produce any effect on the displacement thickness. This implies that the slope of the streamlines v/u near the bottom of region 6 has to coincide with the slope v/u of the streamlines at the outer edge of region 5 (see figure 9). Using expansions (4.15) for region 0 and (4.12)–(4.14) for region 5, the matching procedure results in

$$v_1^* = -\frac{1}{\lambda}\frac{\partial A_1^*}{\partial x_*} - \frac{1}{\lambda}\overline{U}_1[\xi_0(\bar{t}), \overline{X}_0, 0]\frac{\mathrm{d}A_0^*}{\mathrm{d}x_*} \quad \text{at} \quad y_* = 0. \tag{4.21}$$

The boundary-value problem (4.16)–(4.18) for the external inviscid region 6 considered together with (4.7), (4.9)–(4.11) for viscous sublayer 4, constitutes the leading-order interaction problem describing the stationary flow over the roughness, while (4.19)–(4.21) coupled with (4.8)–(4.11) represent the interaction problem for oscillatory perturbations around the roughness.

5. Tollmien–Schlichting wave generation

If the scaled height of the roughness, i.e. $F(x_*)$ in (2.9), is $O(1)$, the leading-order stationary perturbations are governed by (4.7) with (4.9) and (4.10). Such nonlinear and complicated flow fields, which can involve separation phenomena, require a fully numerical investigation. Although the problem of receptivity in the presence of the backflow is interesting, it is beyond the objectives of the present investigation. On the other hand, if the characteristic height of the roughness may be taken as a small parameter, subsequent linearization leads to an analytic solution. We therefore write the roughness geometry as

$$F(x_*) = hF^*(x_*), \tag{5.1}$$

and allow $h \to 0$.

In accordance with the representation (5.1), the solution for leading-order stationary equations (4.7), (4.9)–(4.11) in the near-wall region 4 (figure 9) may be written as

$$\left.\begin{aligned} U_0^* = \lambda Y_* + h\lambda^{1/4}U_0(x, Y) + \ldots, \quad V_0^* = h\lambda^{3/4}V_0(x, Y) + \ldots, \\ P_0^* = h\lambda^{1/2}P_0(x) + \ldots, \quad A_0^* = h\lambda^{1/4}A_0(x) + \ldots, \\ x_* = \lambda^{-5/4}x, \quad Y_* = \lambda^{-3/4}Y, \quad F^* = \lambda^{-3/4}f(x). \end{aligned}\right\} \tag{5.2}$$

Here asymptotic expansions valid for small h have been combined with an affine transformation to exclude the constant λ from the equations for both the viscous near-wall region 4 and the external inviscid region 6 (see figure 9). The corresponding expressions for region 6 are

$$u_0^* = h\lambda^{1/2}u_0(x,y) + \ldots, \qquad v_0^* = h\lambda^{1/2}v_0(x,y) + \ldots,$$

$$p_0^* = h\lambda^{1/2}p_0(x,y) + \ldots, \qquad y_* = \lambda^{-5/4}y. \tag{5.3}$$

Substitution of (5.2) into (4.7), (4.9)–(4.11) results in

$$\left.\begin{gathered} Y\frac{\partial U_0}{\partial x} + V_0 = -\frac{\mathrm{d}P_0}{\mathrm{d}x} + \frac{\partial^2 U_0}{\partial Y^2}, \qquad \frac{\partial U_0}{\partial x} + \frac{\partial V_0}{\partial Y} = 0, \\ U_0 = -f(x), \quad V_0 = 0 \quad \text{at} \quad Y = 0, \\ U_0 \to 0 \quad \text{as} \quad x \to -\infty; \quad U_0 = A_0(x) + \ldots \text{as} \quad Y \to \infty. \end{gathered}\right\} \tag{5.4}$$

Equations (5.4) do not form a closed boundary-value problem. They must be augmented with

$$\left.\begin{gathered} \frac{\partial^2 p_0}{\partial x^2} + \frac{\partial^2 p_0}{\partial y^2} = 0, \\ p_0 \to 0 \quad \text{as} \quad x^2 + y^2 \to \infty, \\ \frac{\partial p_0}{\partial y} = \frac{\mathrm{d}^2 A_0}{\mathrm{d}x^2} \quad \text{at} \quad y = 0, \end{gathered}\right\} \tag{5.5}$$

which may be obtained by substituting (5.3) into (4.16)–(4.18) and subsequent elimination of u_0 and v_0 from the equations of motion.

If the displacement function $A_0(x)$ were known, then equations (5.5) could be used to find the pressure $p_0(x,y)$ everywhere in region 6 and, particularly, at the outer edge of the boundary layer. Since the pressure does not change across the boundary layer, in region 4

$$P_0(x) = p_0(x,0). \tag{5.6}$$

Similarly, to determine the behaviour of non-stationary perturbations in the interaction region, it is necessary to solve the following system for region 4:

$$\left.\begin{gathered} \frac{\partial U_1}{\partial t} + Y\frac{\partial U_1}{\partial x} + V_1 = -\frac{\partial P_1}{\partial x} + \frac{\partial^2 U_1}{\partial Y^2}, \quad \frac{\partial U_1}{\partial x} + \frac{\partial V_1}{\partial Y} = 0, \\ U_1 = V_1 = 0 \quad \text{at} \quad Y = 0, \\ U_1 \to 0 \quad \text{as} \quad x \to -\infty; \quad U_1 \to A_1(t,x) \quad \text{as} \quad Y \to +\infty, \end{gathered}\right\} \tag{5.7}$$

combined with

$$\left.\begin{gathered} \frac{\partial^2 p_1}{\partial x^2} + \frac{\partial^2 p_1}{\partial y^2} = 0, \\ p_1 \to 0 \quad \text{as} \quad x^2 + y^2 \to \infty, \\ \frac{\partial p_1}{\partial y} = \frac{\partial^2 A_1}{\partial x^2} + 2\overline{U}_1(\xi_0, \overline{X}, 0)\frac{\mathrm{d}^2 A_0}{\mathrm{d}x^2} \quad \text{at} \quad y = 0, \end{gathered}\right\} \tag{5.8}$$

via the pressure equality

$$P_1(t,x) = p_1(t,x,0), \tag{5.9}$$

where

$$\bar{t} = \lambda^{-3/2} t.$$

It is seen that the stationary problem (5.4)–(5.6) is similar to the problem considered by Stewartson (1970) and may be solved by means of Fourier transforms. Following Stewartson's argument it can be easily shown that the solution of (5.4)–(5.6) gives

$$A_0^{**}(k) = -\frac{f^{**}(k)}{1 + (ik)^{1/3}|k|\Gamma(\frac{1}{3})/3^{2/3}},$$

where $A_0^{**}(k)$ is the Fourier image of the displacement function

$$A_0^{**}(k) = \frac{1}{(2\pi)^{1/2}} \int_{-\infty}^{\infty} A_0(x) e^{-ikx} dx,$$

and $f^{**}(k)$ is similarly the Fourier image of the wall roughness, and the appropriate root of $(ik)^{1/3}$ is chosen with the branch cut taken along the positive imaginary axis, as standard.

Turning to the unsteady problem (5.7)–(5.9) (remembering that $\overline{U}_1$ in (5.8) is a periodic function of time), and using the substitution $\xi_0(t) = \bar{x}_0 - \lambda^{-3/2} t$ in (3.36) gives

$$\overline{U}_1(\xi_0(t), \overline{X}_0, 0) = \sum_{n=-\infty}^{\infty} \overline{U}_{1n}(\overline{X}_0) e^{in\alpha\bar{x}_0} e^{-in\alpha\lambda^{-3/2}t}. \tag{5.10}$$

Since the problem (5.7)–(5.9) is linear, each mode becomes decoupled, and we may therefore treat each value of n in isolation, or more specifically consider

$$\overline{U}_1(\xi_0(t), \overline{X}_0, 0) = \overline{U}_{1n}(\overline{X}_0) e^{in\alpha\bar{x}_0} e^{-in\alpha\lambda^{-3/2}t} + \overline{U}_{1(-n)}(\overline{X}_0) e^{-in\alpha\bar{x}_0} e^{in\alpha\lambda^{-3/2}t}, \tag{5.11}$$

where $\overline{U}_{1(-n)}$ is the complex conjugate of $\overline{U}_{1n}$, and then (5.11) may be rewritten in the form

$$\overline{U}_1(\xi_0(t), \overline{X}_0, 0) = \mathrm{Re}\left(B e^{i\omega t}\right), \tag{5.12}$$

where Re denotes the real part of the expression in the braces, amplitude B is defined as

$$B = 2\overline{U}_{1(-n)}(\overline{X}_0) e^{-in\alpha\bar{x}_0},$$

and the frequency of oscillation is

$$\omega = n\alpha\lambda^{-3/2}.$$

With the function $\overline{U}_1(\xi_0(t), \overline{X}_0, 0)$ defined by (5.12) and a known leading-order stationary displacement thickness distribution $A_0(x)$, the unsteady interaction problem (5.7)–(5.9) takes the form which may be shown (with the help of the Prandtl transposition theorem) to be equivalent to the problem considered by Terent'ev (1981,1984) in his analysis of Tollmien–Schlichting wave generation by a vibrating wall. The method of Fourier transformations is again applicable.

The unsteady pressure, which arises as a result of the interaction between perturbations of the form (5.12) in the vortex boundary layer and the displacement due to the roughness, may be found from (5.8) to be

$$P_1^{**} = |k| \left(A_1^{**}(k) + 2BA_0^{**}(k)\right). \tag{5.13}$$

After Fourier transformation, equations (5.7) become

$$i\omega U_1^{**} + Y ikU_1^{**} + V_1^{**} = -ikP_1^{**} + \frac{\partial^2 U_1^{**}}{\partial Y^2},$$

$$ik U_1^{**} + \frac{\partial V_1^{**}}{\partial Y} = 0,$$

with

$$\left.\begin{aligned} V_1^{**} = U_1^{**} = 0 \quad \text{at} \quad Y = 0, \\ U_1^{**} \to A_1^{**} + \ldots \quad \text{as} \quad Y \to \infty. \end{aligned}\right\} \tag{5.14}$$

The analysis is routine (see for example Terent'ev 1981, 1984; Goldstein 1985), and may be completed using Airy functions, leading to the result that

$$A_1^{**}(k) = \frac{(ik)^{1/3}|k| \displaystyle\int_{z_0}^{\infty} \mathrm{Ai}(z)\mathrm{d}z}{Q(z_0, k)} 2BA_0^{**}(k), \tag{5.15}$$

where

$$Q(z_0, k) = \mathrm{Ai}'(z_0) - (ik)^{1/3}|k| \int_{z_0}^{\infty} \mathrm{Ai}(z)\mathrm{d}z, \tag{5.16}$$

and $z_0 = \omega/k(ik)^{1/3}$. Knowing $A_0^{**}(k)$ and $A_1^{**}(k)$ it is easy to obtain other flow quantities, for example we may write

$$P_1^{**}(k) = P_{11}^{**}(k) + P_{12}^{**}(k), \tag{5.17}$$

where

$$P_{11}^{**}(k) = 2B|k|A_0^{**}(k), \quad P_{12}^{**}(k) = \frac{\mathrm{i}^{1/3}k^{7/3} \displaystyle\int_{z_0}^{\infty} \mathrm{Ai}(z)\mathrm{d}z}{Q(z_0, k)} 2BA_0^{**}(k). \tag{5.18}$$

In principle, all flow quantities may be calculated by means of inverse Fourier transformation. In particular, the pressure takes the form

$$P_1(t, x) = \mathrm{Re}\left(\mathrm{e}^{\mathrm{i}\omega t} \frac{1}{(2\pi)^{1/2}} \left[\int_{-\infty}^{\infty} P_{11}^{**}(k)\mathrm{e}^{\mathrm{i}kx}\mathrm{d}k + \int_{-\infty}^{\infty} P_{12}^{**}(k)\mathrm{e}^{\mathrm{i}kx}\mathrm{d}k\right]\right). \tag{5.19}$$

Following Terent'ev (1981), we subdivide the contour of integration in (5.19) into two parts, namely the negative real semi-axis C_1 and the positive real semi-axis C_2. Using Cauchy's theorem, we replace the integral along C_1 with the integrals along C_R' and C_1' as shown in figure 10. Correspondingly, the integration along C_2 may be replaced with the integration along C_2' and C_R''. Suppose further that the function $f(x)$, representing the shape of the wall roughness has a Fourier image $f^{**}(k)$ which may be analytically continued from the negative real semi-axis into the region inside the first closed contour and from the positive real semi-axis into the region inside the second contour. In that case the only singularities we have to take into account having changed the integration are the poles of P_{12}^{**} located at points where

$$Q(z_0, k) = 0. \tag{5.20}$$

Equation (5.20) represents a dispersion relation connecting wavenumbers and frequencies of the 'eigen' oscillations of the subsonic boundary layer in the vicinity of the lower branch of the neutral-stability curve (Lin 1946) at large Reynolds number. The properties of relation (5.20) are well-known and may be found, for example, in Zhuk & Ryzhov (1980), Terent'ev (1981), and Duck (1990). It is known that the dispersion relation (5.20) has an infinite set of roots $k_i(\omega)$, all of which except the first, $k_1(\omega)$, being located above the real axis for all ω, and it is $k_1(\omega)$ that is responsible for the generation of Tollmien–Schlichting waves. If ω is smaller than the 'neutral

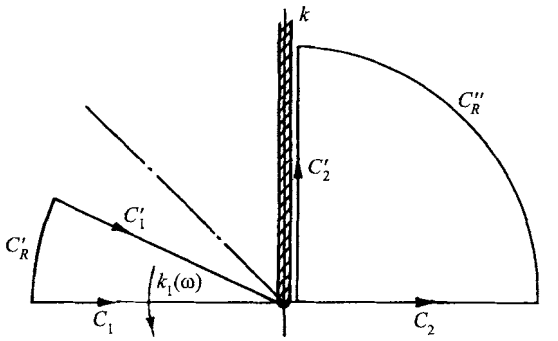

FIGURE 10. Integration contours

stability' value $\omega_* \approx 2.298$, then $k_1(\omega)$ is located above the real axis (see figure 10). But as ω grows the first root $k_1(\omega)$ moves toward the lower half-plane, crossing the real axis at $k_1 \approx -1.0005$ where $\omega = \omega_*$.

It is clear from consideration of the above that the integration along the negative real axis in I_1 may be replaced by an integration along the contour C_1' which always contains the 'unstable' root $k_1(\omega)$ (but none of the other, stable roots). The contribution from this pole is

$$P_{ts} = \mathrm{Re}\left((2\pi)^{1/2} \frac{\mathrm{i}^{1/3} k_1^{7/3} \int_{z_1}^{\infty} \mathrm{Ai}(z)\mathrm{d}z}{(dQ/dk_1)(z_1, k_1)} 2BA_0^{**}(k_1) \mathrm{e}^{\mathrm{i}(\omega t + k_1 x)} \right),$$

where

$$\frac{\mathrm{d}Q}{\mathrm{d}k_1}(z_1, k_1) = \tfrac{2}{3}\mathrm{i}^{1/3} k_1^{1/3} \left(2\int_{z_1}^{\infty} \mathrm{Ai}(z)\mathrm{d}z + z_1 \mathrm{Ai}(z_1)(1 - \frac{\omega}{k_1^2}) \right),$$

$$z_1 = \frac{\omega}{k_1(\omega)} (\mathrm{i}k_1(\omega))^{1/3},$$

and

$$A_0^{**}(k_1) = -\frac{f^{**}(k_1)}{1 - \mathrm{i}^{1/3} k_1^{4/3} \Gamma(1/3)/3^{2/3}}.$$

6. Concluding remarks

The analysis in the present paper reveals that the generation of Tollmien–Schlichting waves by free-stream turbulence differs considerably from their generation by sound (see Ruban 1984 and Goldstein 1985). Acoustic waves are known to exist due to the periodic compression and expansion of the medium, and so the pressure oscillations are an intrinsic feature of a flow involving acoustic perturbations. These easily penetrate into the boundary layer causing the longitudinal velocity component to oscillate in the Stokes layer near the flat-plate surface. Nonlinear interaction of the Stokes layer oscillations with stationary flow perturbations provoked by wall roughness in the viscous sublayer of the triple-deck structure leads to Tollmien–Schlichting wave generation.

Vorticity waves do not produce pressure oscillations (at least, to the leading order of magnitude), and so do not cause perturbations inside the boundary layer. Velocity

oscillations at its outer edge cannot penetrate into the bulk of the boundary layer. These decay rapidly in the intermediate shear layer between the boundary layer and external inviscid flow. This shear layer occupies a strip of characteristic thickness $O[(Re \log Re)^{-1/2}]$ at a distance $O[Re^{-1/2}(\log Re)^{1/2}]$ from the wall. As a result the viscous sublayer (the lower deck of the triple-deck structure) on the surface of the wall roughness is not affected by the vorticity waves. On the other hand, the roughness produces the flow perturbations not only inside the boundary layer, but also outside the boundary layer, in the upper deck of the triple-deck structure. These stationary perturbations interact with the velocity oscillations in the vorticity waves leading to Tollmien–Schlichting wave generation.

Another interesting point is the existence of the 'turbulence deformation layer', where the nonlinear process of the vorticity field modification near the flat-plate surface takes place. Ultimately, this leads to a shock/discontinuity type singularity in the flow some distance downstream of the plate leading edge. There has been much interesting work carried out on the occurrence/non-occurrence of singularities of the Euler equations (see for example Tanveer & Speziale 1992), although the location of the (effective) stagnation point on the flow boundary does have a profound effect on the flow. This singularity may be interpreted as the formation of a strong vortex, and it is likely that its influence on the flow in the boundary layer may cause an 'abrupt' laminar-turbulent transition. Since the slow variable $\bar{X}$ in equation (3.10) is related to the amplitude ϵ of the free-stream perturbations by equation (3.2), the 'soft' transition via generation of Tollmien–Schlichting waves must be expected for small ϵ, while the 'abrupt' transition is more likely to occur when ϵ is relatively high. Another point regarding this region is that there is some possibility that it may be linked in some way with the eigensolutions found by Brown & Stewartson (1973*a*,*b*), pertinent to eigensolutions concentrated in the outer region of the boundary layer. This will be the subject of further investigation.

The work of A.I.R. was supported by United Technologies Research Center and by EPSRC. The work of C.N.Z. was supported by United Technologies Research Center. A number of computations were performed with EPSRC-funded equipment.

REFERENCES

Bodonyi, R. J., Welch, W. J. C., Duck, P. W. & Tadjfar, M. 1989 A numerical study of the interaction between unsteady free-stream disturbances and localized variations in surface geometry. *J. Fluid Mech.* **209**, 285.

Brown, S. N. & Stewartson, K. 1973*a* On the propagation of disturbances in a laminar boundary layer I. *Proc. Camb. Phil. Soc.* **73**, 493.

Brown, S. N. & Stewartson, K. 1973*b* On the propagation of disturbances in a laminar boundary layer II. *Proc. Camb. Phil. Soc.* **73**, 503.

Dryden, H. L. 1956 Recent investigations of the problem of transition. *Z. Flugwiss.* **4**, 89.

Duck, P. W. 1985 Laminar flow over unsteady humps: the formation of waves. *J. Fluid Mech.* **160**, 465.

Duck, P. W. 1988 The effect of small surface perturbations on the pulsatile boundary layer on a semi-infinite flat plate. *J. Fluid Mech.* **197**, 259.

Duck, P. W. 1990 Triple-deck flow over unsteady surface disturbances: the three-dimensional development of Tollmien–Schlichting waves. *Computers Fluids* **18**, 1.

Fedorov, A. V. 1982 Generation of instability waves in a boundary-layer flow of compressible gas exposed to an acoustic field. *Numer. Meth. Continuum Mech. (Novosibirsk)* **13**, 106.

Goldstein, M. E. 1985 Scattering of acoustic waves into Tollmien–Schlichting waves by small streamwise variation in surface geometry. *J. Fluid Mech.* **154**, 509.

GOLDSTEIN, M. E. 1983 The evolution of Tollmien–Schlichting waves near a leading edge. *J. Fluid Mech.* **127**, 59.

GOLDSTEIN, M. E. & LEIB, S. J. 1993*a* Three-dimensional boundary-layer instability and separation induced by small amplitude streamwise vorticity in the upstream flow. *J. Fluid Mech.* **246**, 21.

GOLDSTEIN, M. E. & LEIB, S. J. 1993*b* A note on the distortion of a flat plate boundary layer by free-stream vorticity normal to the plate. *J. Fluid Mech.* **248**, 531.

GOLDSTEIN, M .E., LEIB, S. J. & COWLEY, S. J. 1992 Distortion of a flat plate boundary layer by free-stream vorticity normal to the plate. *J. Fluid Mech.* **237**, 231.

GULIAEV, A. N., KOZLOV, V. E., KUZNETSOV, V. R., MINEEV, B. I. & SECUNDOV, A. N. 1989 Interaction of a laminar boundary layer with external disturbances. *Izv. Akad. Nauk SSSR Mekh. Zhid. Gaza* **6**, 55.

HUNT, J. C. R. & GRAHAM, J. M. R. 1978 Free-stream turbulence near plane boundaries. *J. Fluid Mech.* **84**, 209.

KERSCHEN, E. J. 1991 *Linear and Nonlinear Receptivity to Vertical Free-Stream Disturbances.* ASME FED, *vol.* 114, p. 43.

LIN, C. C. 1946 On the stability of two-dimensional parallel flows. Part 3. Stability in a viscous fluid. *Q. Appl. Maths* **3**, 277.

MORKOVIN, M. V. 1969 Critical evaluation of transition for laminar to turbulent shear layers with emphasis on hypersonically traveling bodies. *Air Force Flight Dynamics Laboratory Rep.* AFFDL-TR-68-149.

RUBAN, A. I. 1984 On Tollmien–Schlichting Wave Generation by Sound. *Izv. Akad. Nauk SSSR Mekh. Zhid. Gaza* **5**, 44.

RYZHOV, O. S. & TIMPEEV, O. A. 1995 Interaction of a potential vortex with a local roughness on a smooth surface. *J. Fluid Mech.* **287**, 21–33.

SCHUBAUER, G. B. & SKRAMSTED, H. K. 1948 Laminar Boundary-Layer Oscillations and Transition on a Flat Plate. *NACA Rep.* 909.

SMITH, F. T. 1979 On the non-parallel flow stability of the Blasius boundary layer. *Proc. R. Soc. Lond.* A **366**, 91.

SMITH, F. T., DOORLY, D. J. & ROTHMAYER A. P. 1990 On displacement-thickness, wall-layer and mid-flow scales in turbulent boundary layers, and slugs of vorticity in channel and pipe flows. *Proc. R. Soc. Lond.* A **428**, 255.

STEWARTSON, K. 1970 On laminar boundary layers near corners. *Q. J. Mech. Appl. Maths* **23**, 137.

SYCHEV, V. V., RUBAN, A. I., SYCHEV, VIC. V. & KOROLEV, G. L. 1987 *Asymptotic Theory of Separated Flows.* Moscow: Nauka.

TANVEER, S. & SPEZIALE, C. G. 1992 Singularities of the Euler equation and hydrodynamic stability. *ICASE Rep.* 92–54.

TERENT'EV, E. D. 1981 Linear problem for vibration in subsonic boundary layer. *Prikl. Mat. Mech.* **45**, 1049.

TERENT'EV, E. D. 1984 Linear problem for vibration performing harmonic oscillations with supercritical frequency in subsonic boundary layer. *Prikl. Mat. Mech.* **48**, 264.

ZHUK, V. I. & RYZHOV, O. S. 1980 Free interaction and stability of boundary layer in incompressible fluid flow. *Proc. Akad. Nauk SSSR* **253**, 1326.